UNCLASSIFIED

SECURITY CLASSIFICATION OF THIS PAGE *(When Data Entered)*

REPORT DOCUMENTATION PAGE		READ INSTRUCTIONS BEFORE COMPLETING FORM
1. REPORT NUMBER NORDA Report 54	2. GOVT ACCESSION NO.	3. RECIPIENT'S CATALOG NUMBER
4. TITLE *(and Subtitle)* Climatological Flux Estimates in the Mediterranean Sea: Part I. Winds and Wind Stresses		5. TYPE OF REPORT & PERIOD COVERED Final 6. PERFORMING ORG. REPORT NUMBER
7. AUTHOR(s) Paul W. May		8. CONTRACT OR GRANT NUMBER(s)
9. PERFORMING ORGANIZATION NAME AND ADDRESS Naval Ocean Research and Development Activity NSTL Station, Mississippi 39529		10. PROGRAM ELEMENT, PROJECT, TASK AREA & WORK UNIT NUMBERS 6.2759
11. CONTROLLING OFFICE NAME AND ADDRESS Naval Ocean Research and Development Activity NSTL Station, Mississippi 39529		12. REPORT DATE October 1982 13. NUMBER OF PAGES 59
14. MONITORING AGENCY NAME & ADDRESS*(if different from Controlling Office)*		15. SECURITY CLASS. *(of this report)* UNCLASSIFIED 15a. DECLASSIFICATION/DOWNGRADING SCHEDULE

16. DISTRIBUTION STATEMENT *(of this Report)*

Distribution Unlimited

17. DISTRIBUTION STATEMENT *(of the abstract entered in Block 20, if different from Report)*

18. SUPPLEMENTARY NOTES

19. KEY WORDS *(Continue on reverse side if necessary and identify by block number)*

Mediterranean Sea
winds
wind stresses
wind systems
Mistral
Bora
Etesian
climatological flux

20. ABSTRACT *(Continue on reverse side if necessary and identify by block number)*

Climatological wind stress averages have been calculated for the entire Mediterranean Sea for one degree longitude squares. The individual stresses were estimated from ship observations of wind speed and wind direction using a quadratic stress law with variable drag coefficient. Individual stresses were averaged by month over the 20-year base period, 1950-1970, to obtain the climatology. Smoothed versions of the monthly wind stress estimates, appropriate for forcing numerical models, were also calculated.

(continued on next page)

DD FORM 1 JAN 73 1473 EDITION OF 1 NOV 65 IS OBSOLETE
S/N 0102-LF-014-6601

UNCLASSIFIED

SECURITY CLASSIFICATION OF THIS PAGE *(When Data Entered)*

(continued from Block 20. Abstract)

Wind stresses exhibit the major wind patterns that are well-known features of the Mediterranean circulation. The Mistral, Bora, and Etesian wind systems are the most evident of the area's features. The seasonal cycles, the curl, and the variance of the wind stresses are presented. Several interesting aspects of the relationship of the Mistral to the formation of bottom water in the Golfe du Lion region are discussed.

NORDA Report 54

Climatological Flux Estimates in the Mediterranean Sea: Part I. Winds and Wind Stresses

Paul W. May

Numerical Modeling Division
Ocean Science and Technology Laboratory

October 1982

Naval Ocean Research and Development Activity
NSTL Station, Mississippi 39529

Foreword

As the accuracy and utility of numerical ocean models increases, the need arises for realistic atmospheric forcing functions. Since the wind stress and heat flux are the most important of the oceanic forcing functions this study aims to develop one such forcing field, the wind stress, for the Mediterranean Sea. A knowledge of the climatological wind stress fields is an essential step toward determining and understanding the wind-driven circulation of any ocean region, especially the Mediterranean Sea where atmosphere-ocean interaction is so important.

G.T. Phelps, Captain, USN
Commanding Officer, NORDA

Executive Summary

Climatological wind stress averages have been calculated for the entire Mediterranean Sea for one degree latitude by one degree longitude squares. The individual stresses were estimated from ship observations of wind speed and wind direction using a quadratic stress law with variable drag coefficient. Individual stresses were averaged by month over the 20-year base period, 1950-1970, to obtain the climatology. Smoothed versions of the monthly wind stress estimates, appropriate for forcing numerical models, were also calculated.

Wind stresses exhibit the major wind patterns that are well-known features of the Mediterranean circulation. The Mistral, Bora, and Etesian wind systems are the most evident of the area's features. The seasonal cycles, the curl, and the variance of the wind stresses are presented. Several interesting aspects of the relationship of the Mistral to the formation of bottom water in the Golfe du Lion region are discussed.

Acknowledgments (U)

This work was supported during FY82 by the Naval Air Systems Command under program element 6.2759 and task number RF59-557 (Exploratory Development in Ocean Forecasting). The project manager, Dr. Steve Piacsek, provided the author with a great deal of encouragement, as did Valentine Worthington of the Woods Hole Oceanographic Institution. This work also owes much to the efforts of Andrew Bunker.

Contents

Illustrations

Illustrations

Illustrations

Climatological Flux Estimates in the Mediterranean Sea: Part I. Winds and Wind Stresses

I. Introduction

The climate of the Mediterranean Sea, particularly the wind field, is perhaps the most studied of all the world's oceans. Minoan and Phoenecian captains were undoubtedly aware of the local wind patterns when they plied the Great Sea nearly 5,000 years ago. This seafaring tradition was continued, in turn, with the Greeks, the Romans, and the Arabs.

Modern man, while less dependent on the wind as a means of propelling commerce, has found the interaction of atmosphere with ocean that occurs in the Mediterranean a compelling subject for study. Wind-driven surface currents transport and diffuse pollutants throughout the limited volume of an almost completely enclosed basin. The exchange of water with the rest of the world's oceans that does take place is largely a consequence of the patterns of evaporation over the entire Mediterranean. The interactions of atmosphere and ocean also result in the formation of deep water masses in the Mediterranean that, in turn, affect the hydrography of the world's oceans.

As part of the effort to understand atmosphere-ocean interactions in the Mediterranean Sea, this exposition focuses on the climatology of winds and wind stresses of the region. This study differs from other similar works in several important ways:

- Unlike Markgraf and Niederschlag (1961) and comparable weather atlases, wind stresses, not winds, are the primary product of interest.

- This study uses an averaging element that is 1° latitude by 1° longitude, not the somewhat standard 5°x5° or 10°x10°, or the irregular regions of Bunker and Goldsmith (1979).

- These calculations use more modern parameterizations than were available to previous authors (e.g., Hellerman, 1965).

- Average stress is calculated from individual stresses, not from averaged winds (as in Hastenrath and Lamb, 1978).

- Calculations are performed on a 20-year base period, 1950-1970.

The primary purpose behind this effort was to develop realistic wind forcing for use in numerical ocean modeling.

II. Data and Methods

The data used in the wind stress calculations were obtained from the National Climatic Center's Tape Data Family-11 (TDF-11). The TDF-11 series is a collection of world-wide surface marine observations made by ships of opportunity. Most records contain observed values of the quantities necessary for computing wind stresses from a bulk formula, namely: wind speed, wind direction, air temperature, sea-surface temperatures and sea level pressure. The data are sorted by Marsden squares, eight of which cover the Mediterranean Sea (Fig. 1). About 1.2 million individual ship observations spanning the period 1937 to 1973 were available for this study.

Because of uneven data coverage of some Marsden squares, a 20-twenty year period from 1 January 1950 to 1 January 1970 was selected for all averaging operations. This period has relatively uniform data for all Marsden squares and for all years, whereas earlier years are sparsely sampled due to World War II, and later years were not archived completely when the data was purchased.

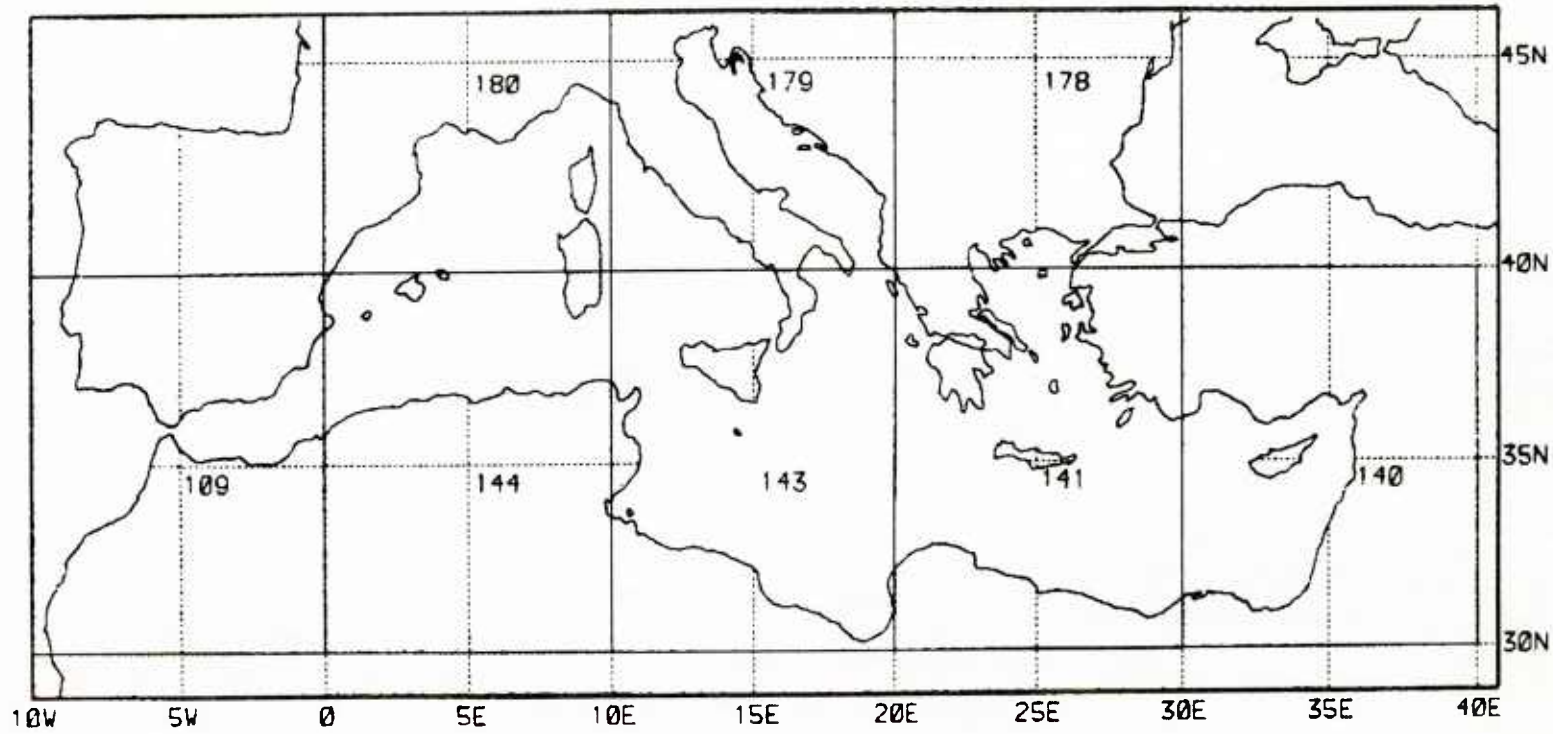

Figure 1. Map of the Mediterranean Sea with Marsden square designations

Given the volume of data available during the 1950s and 1960s, twenty years also seems to be the minimum time necessary to obtain stable averages on one degree grid elements. It is hoped that this will be a useful period for comparison with other climatological averages.

Although the National Climatic Center has edited the data, further screening was performed to detect and eliminate erroneous data values. Observations of wind speed in excess of 40 meters per second (m/sec) and wind directions not in the range from 0 to 360 were excluded from the calculations. Records with missing information and reported positions not in or near the Mediterranean Sea were ignored. As a result of the editing and the limited averaging period about, 800,000 ship reports were used for the final calculations.

To compute wind stresses from the ship observations the well-known nonlinear bulk formula for turbulent momentum transfer was used:

$$\tau = \rho C_d U^2$$

where

τ is the wind stress,
ρ is the air density,
C_d is the drag coefficient, and
U is the wind speed.

In its most complete form, ρ is a function of air temperature and pressure, and C_d is a function of wind speed and stability.

Following standard practice, the drag coefficient is calculated as the product of its value under neutrally stable conditions and a stability dependent term,

$$C_d(U,S) = F(S)\ C_n(U).$$

The functional form of the neutral drag coefficient has received much attention in recent years (Garratt, 1977). Although opinion is far from unanimous, most investigators find a linear relationship between the neutral drag coefficient and the wind speed. The relationship used for the wind stress calculations in the Mediterranean is

$$C_n(U) = 0.9 + 0.06\ U.$$

This form was chosen somewhat arbitrarily as a compromise among the several forms shown in Figure 2. The scatter of the observations is sufficient to mask any differences between the various functional forms.

The effects of stability are included by using a parameterization due to Kondo (1975) which uses the air-sea temperature difference and wind speed to calculate a stability parameter:

$$F(S) = \begin{cases} 0.1 + 0.03\ S' + 0.9\ \exp(4.8\ S') & S' < 0 \text{ Stable,} \\ 1.0 + 0.47\ \sqrt{S'} & S' > 0 \text{ Unstable,} \end{cases}$$

where

$$S' = S|S|/(|S| + 0.01), \text{ and}$$
$$S = (T_{air} - T_{sea})/U^2.$$

Comparisons of stress averages calculated with the stability correction and those calculated with no correction show that stability for Mediterranean Sea climatology is rather unimportant; differences in the stresses amounted to less than 3%.

Although a variable density, ρ, was calculated using the ideal gas law, comparisons with constant density calculations show that its effect on the averaged stresses was negligible (<1% differences).

Because of the nonlinear form of the drag law, stress averages are computed from the sum of individual stresses--not from averaged winds. Comparisons show that while directional differences between the two techiques are small, large (a factor of 2-5) stress magnitude differences do occur. These magnitude differences are a reflection of the wind variability and are virtually uncorrectable.

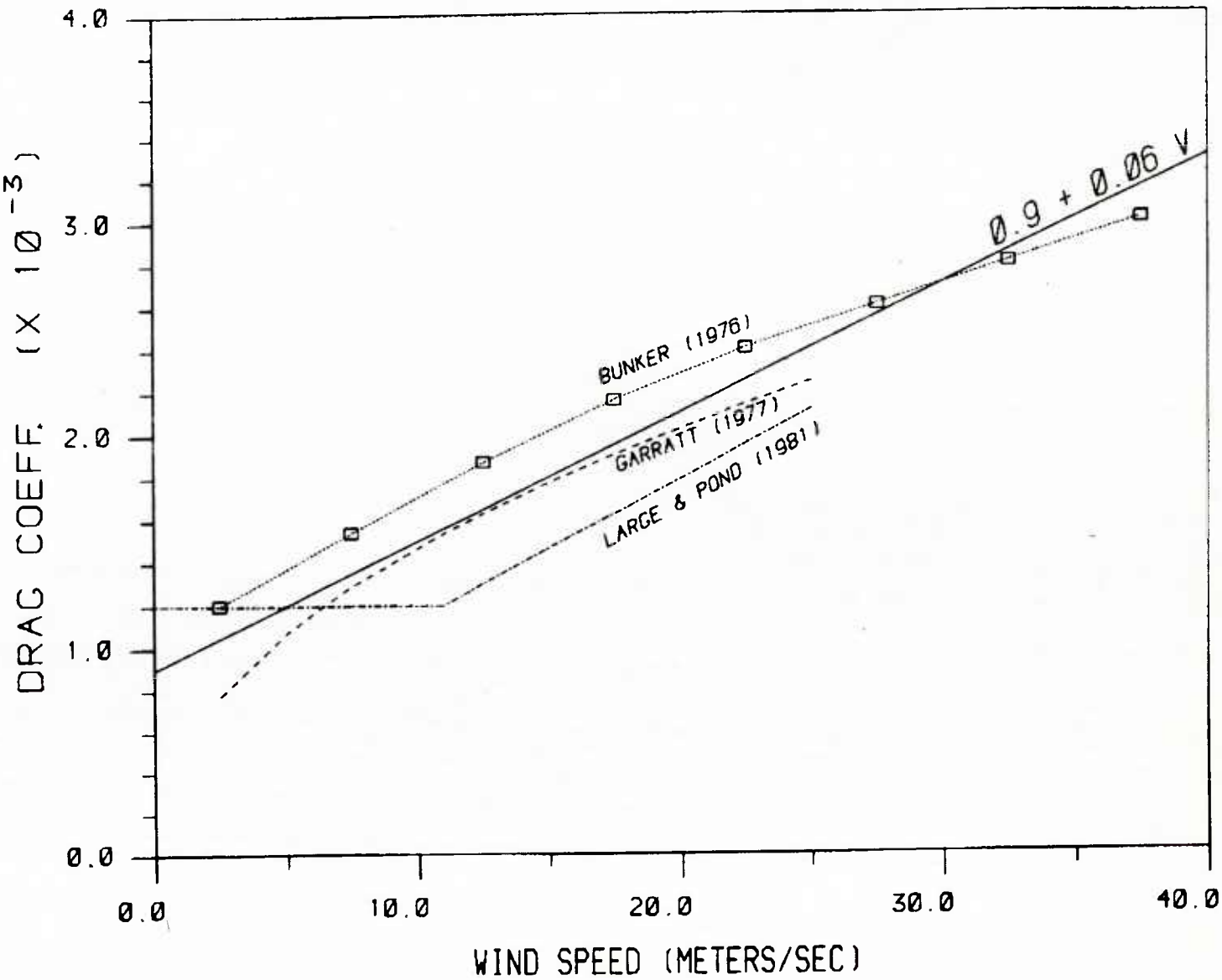

Figure 2. Comparison of various functional forms of the drag coefficient, C_n

The procedure used to calculate a vector average stress from an observation of wind speed and direction was to compute a stress magnitude from the wind speed alone, and then decompose it into East-West and North-South components using the wind direction. The components were then accumulated for one degree latitude/longitude "squares" for each month of the year over the 20-year base period. Thus, for example, the January monthly average is the average of 20 Januarys. The 20-year monthly averages were used to form seasonal averages and an annual average as shown in the flow chart of Figure 3. Averaging in this manner eliminates seasonal biases which may develop when certain seasons have a larger number of data points than others.

The choice of a spacial averaging interval (1° x 1°) is partially based on a study of the wave number spectrum of the wind stress in the Ionian and Levantine basins of the Mediterranean. Stresses were calculated along ten East-West lines running from about 10E to 36E, using 0.2° x 0.2° averaging boxes. The lines were spaced at 0.2° intervals meridionally starting at 33N. The region of coverage is shown in Figure 4. The ten series, consisting of 128 point averages of x and y stress, were processed by removing the mean of each sequence, tapering the series with a "ten percent window," and then calculating the vector wave number spectrum of each. The ten spectra were then averaged to give the spectrum shown in Figure 5.

This spectrum represents the x-direction wavenumber spectrum of the averaged wind stress for the southeastern Mediterranean Sea. It shows a rapid decrease in energy content for wavelengths less than about 250 kilometers (km) followed by a region of flattening, which is interpreted as the noise level of the averaging process. While this wavenumber spectrum is probably not representative of the entire Mediterranean, it does crudely indicate the limits of resolution achievable in this analysis.

Noting that 0.2° boxes are too small (energy being dominated by noise) and that 5° boxes are too large (energy levels indicate presence of signal) a compromise averaging region of one degree latitude by one degree longitude was chosen for this study. This choice is further supported by Saunders (1976), who found that wind stress averages over regions greater than that covered by a 1° x 1° square resulted in underestimates of wind stress curl.

As with short temporal averages, small-scale spacial averages reduce biases that can arise when the averaging region has varying observational densities coupled with gradients of the properties being averaged (Weare and Strub, 1981). The price paid for reduced bias and more accurate gradient calculation is lower stability in estimates of the average due to the smaller number of observations for each averaging interval. In calculating averages over regions with greatly disparate data densities, the tradeoff between finer resolution and greater statistical stability is a difficult process to optimize.

Since one objective of this work was to produce wind fields suitable for forcing numerical models, smoothed versions of the wind stress fields have also been calculated. Smoothing emphasizes the stability of the stress fields rather than the resolution. The smoothing operation consists of applying spacial and temporal filters to the monthly averaged fields.

The temporal filter was a simple three-point, observation-weighted nonrecursive system of the form:

$$F'(i) = (W\,N(i-1) + N(i)\,F(i) + W\,N(i+1)\,F(i+1))/D$$

where

$W = 0.3$,
$N(i)$ = the number of observations during month i

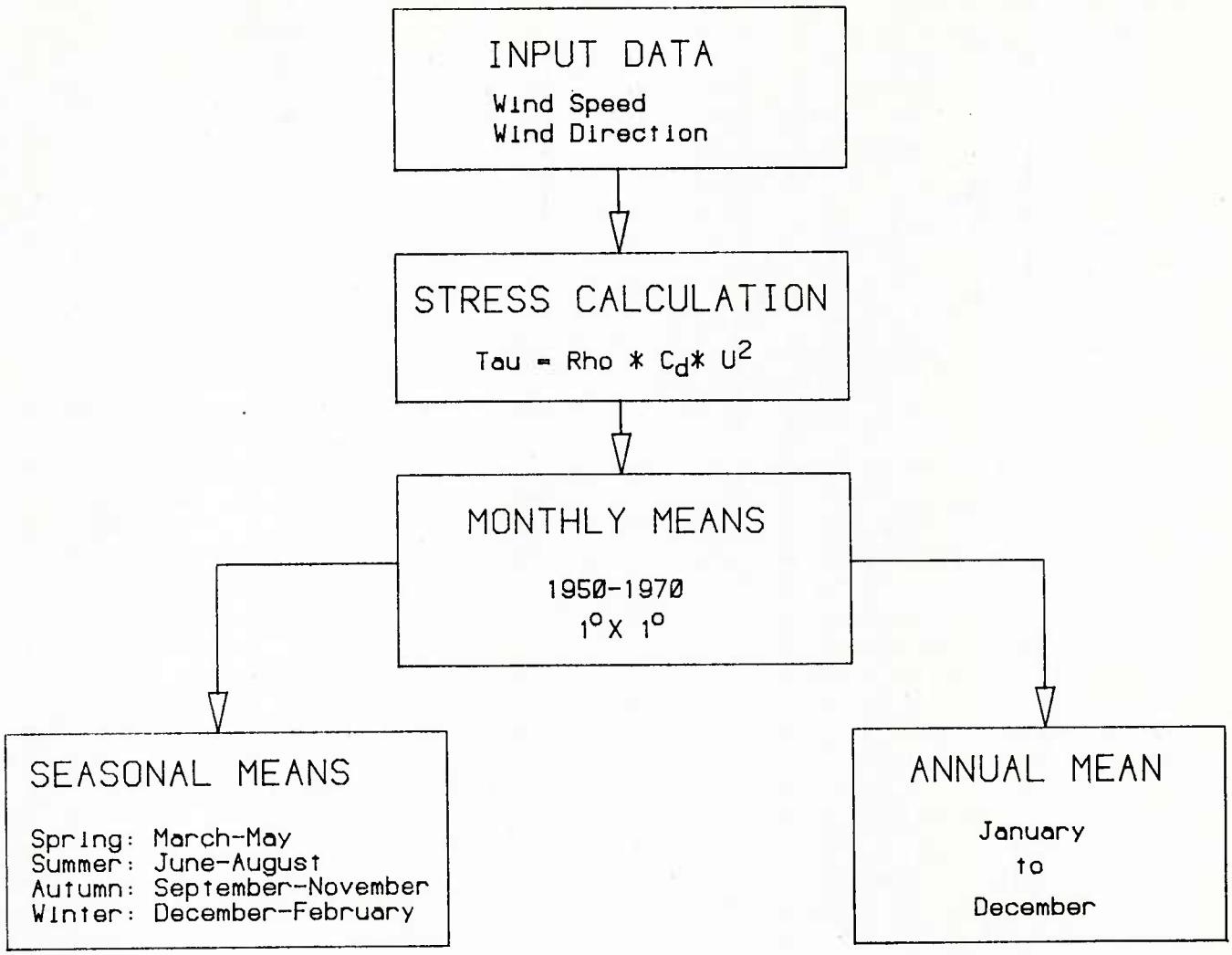

Figure 3. Flow chart of the calculations

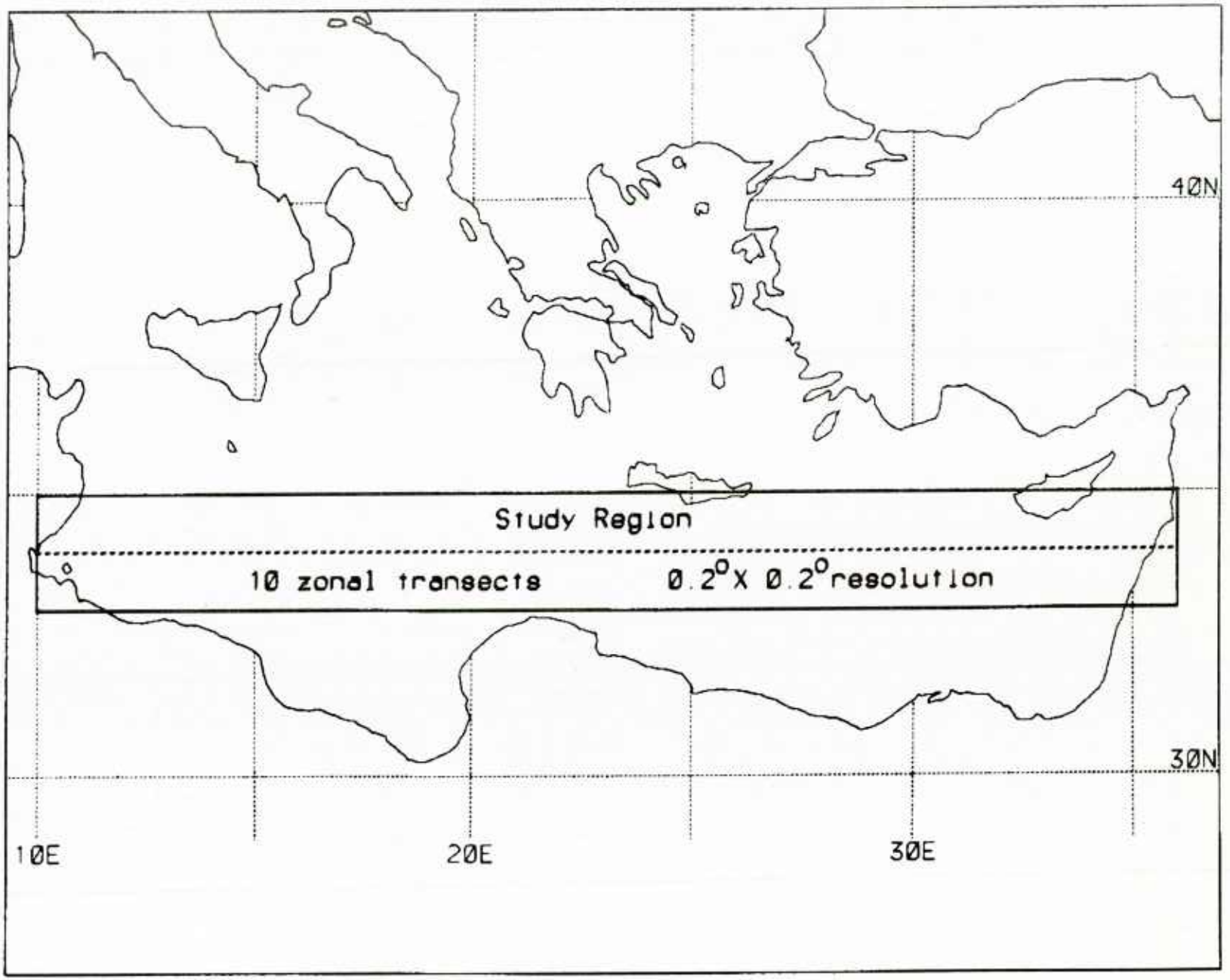

Figure 4. Map of the wind stress wavenumber spectrum study region

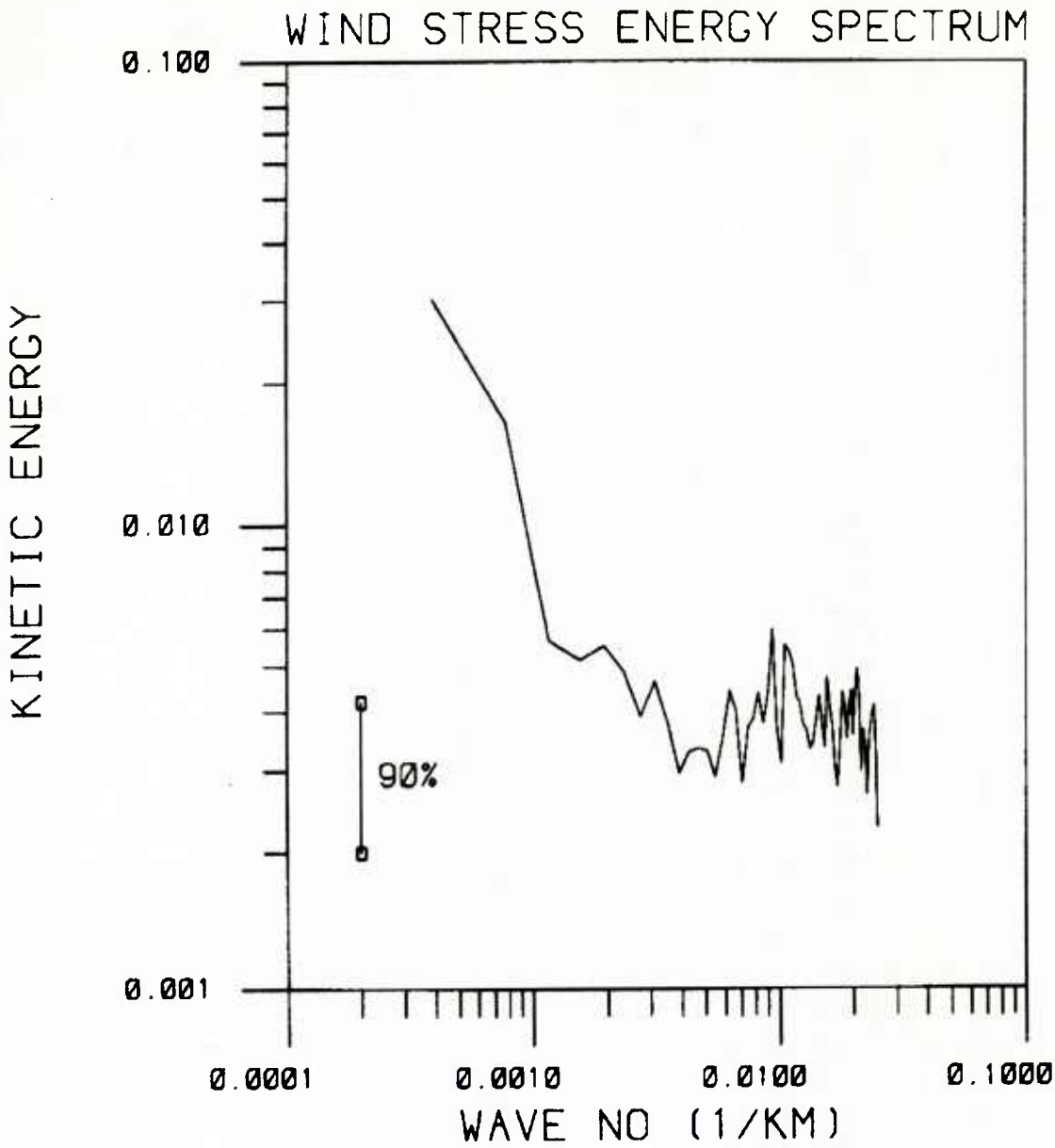

Figure 5. Vector wavenumber spectrum of the wind stress with 0.2 degree resolution

F(i) = the unfiltered parameter at month i,
F'(i) = the filtered parameter at month i,
D = the normalizing factor, W N(i-1) + N(i) + W N(i+1).

This filter reduces the amplitude of 2.5 month fluctuations by half if the number of observations are the same during adjacent months. If the number of observations differ, the filter slightly favors the estimate based on the largest number of observations; thus introducing small (<30°) phase shifts.

The weighting scheme of the spacial filter is shown in Figure 6. This filter also weights estimates in proportion to the number of observations. It has circular symmetry and reduces the amplitude of the 200 km fluctuations by half if the number of observations are comparable at all nine grid elements. This filter produces slight spacial phase shifts when observations are not uniform, since the weights spread data information from well-sampled to poorly sampled points.

A comparison of the wind stress averages calculated without modification and those that were filtered can be made by comparing Figure 7 with Figure 12. The difference between the two is generally small; however, regions with strong gradients and regions with limited observational data bases show significant differences in the filtered fields. These differences are usually a reduction of vector magnitude but occasionally consist of vector rotations (<10°). In all cases the differences are not noticeable over large regions--they are mainly confined to single points where the number of observations was significantly smaller than adjacent points.

The sources of error in climatological flux estimates have been discussed by Bunker (1976). It is estimated that the measurements of wind speed, wind direction, and other quantities have uncertainties of around 10% due to instrumental errors and other factors such as fair weather bias. In addition the calculation of stress with a bulk formula probably introduces uncertainties of not more than 20%. While the filtering process does admit more uncertainty (estimated to be about 5%), it is small compared to the other factors.

Calculations were performed on the Texas Instruments Advanced Scientific Computer at the Naval Research Laboratory. Careful coding and the vector processing feature of this machine allowed very efficient handling of the large amounts of data available; calculations for one Marsden square typically used about $10.00 worth of computer time.

III. Wind and Wind Stresses

The primary product of these calculations is a set of climatological wind stress estimates for each month of the year over the entire Mediterranean Sea. These can be quickly summarized by considering the annual mean of the stress field and related quantities, and the annual cycle as seen in the seasonal averages. A brief description of these fields and the amount of data that was used is presented here.

Figure 8 shows that the distribution of observations roughly follows shipping lanes in the Mediterranean Sea. The straits of Gibraltar and Sicily as well as the regions around the ports of Monaco and Naples have the highest number of observations (10,000-12,000) during the 20-year period. In contrast, the Adriatic and offshore regions near Libya are large areas where relatively few observations (<1000) were made.

The annual mean wind field (Fig. 9) is dominated by regional wind systems having speeds which range from 5-7 m/sec. The most obvious of these systems exists in the northwestern corner of the Mediterranean (Golfe du Lion) and in the Aegean Sea. Both are well-known features of the region.

Markgraf and Niederschlag (1961) have performed a similar study of the mean

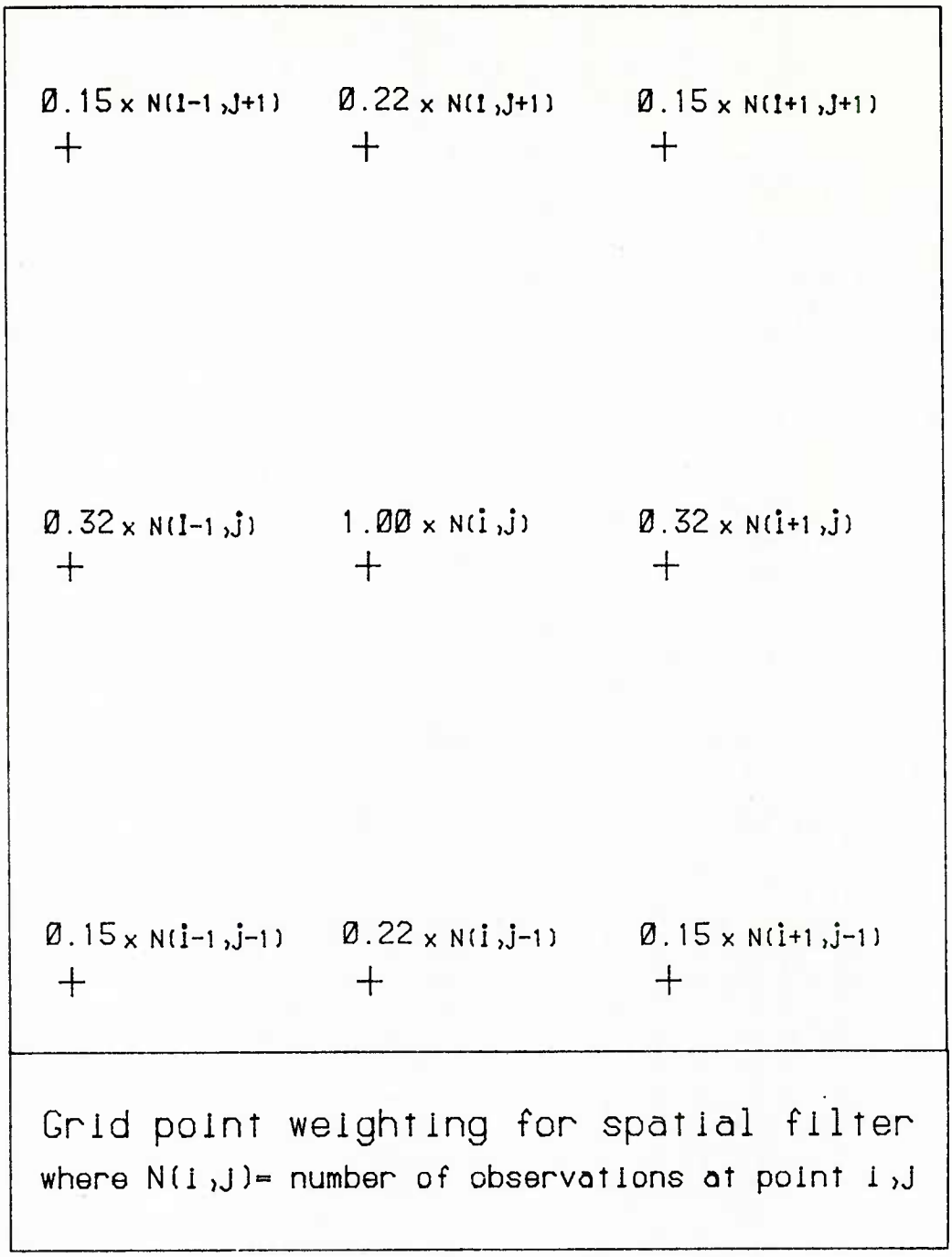

Figure 6. Weighting factors for two dimensional, nine point spatial filter

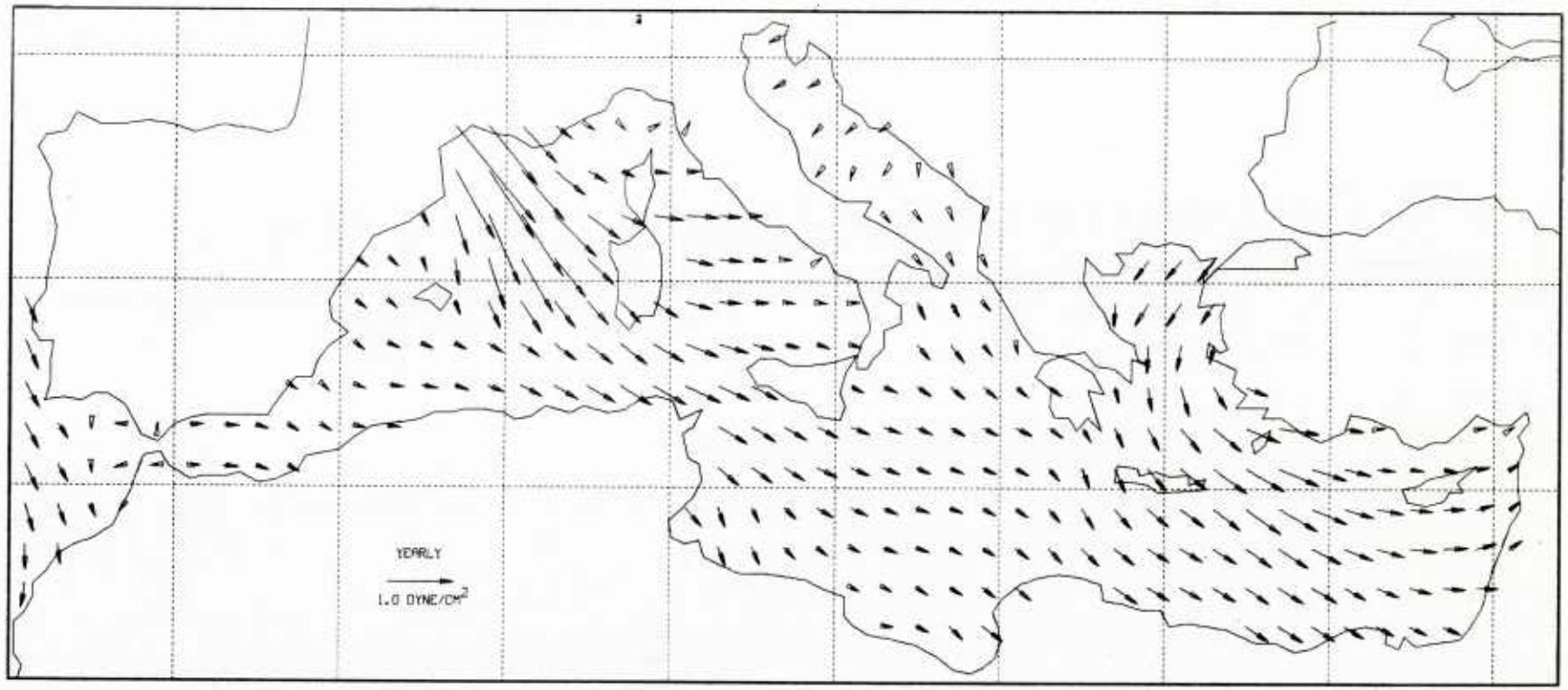

Figure 7. Filtered annual wind stress average

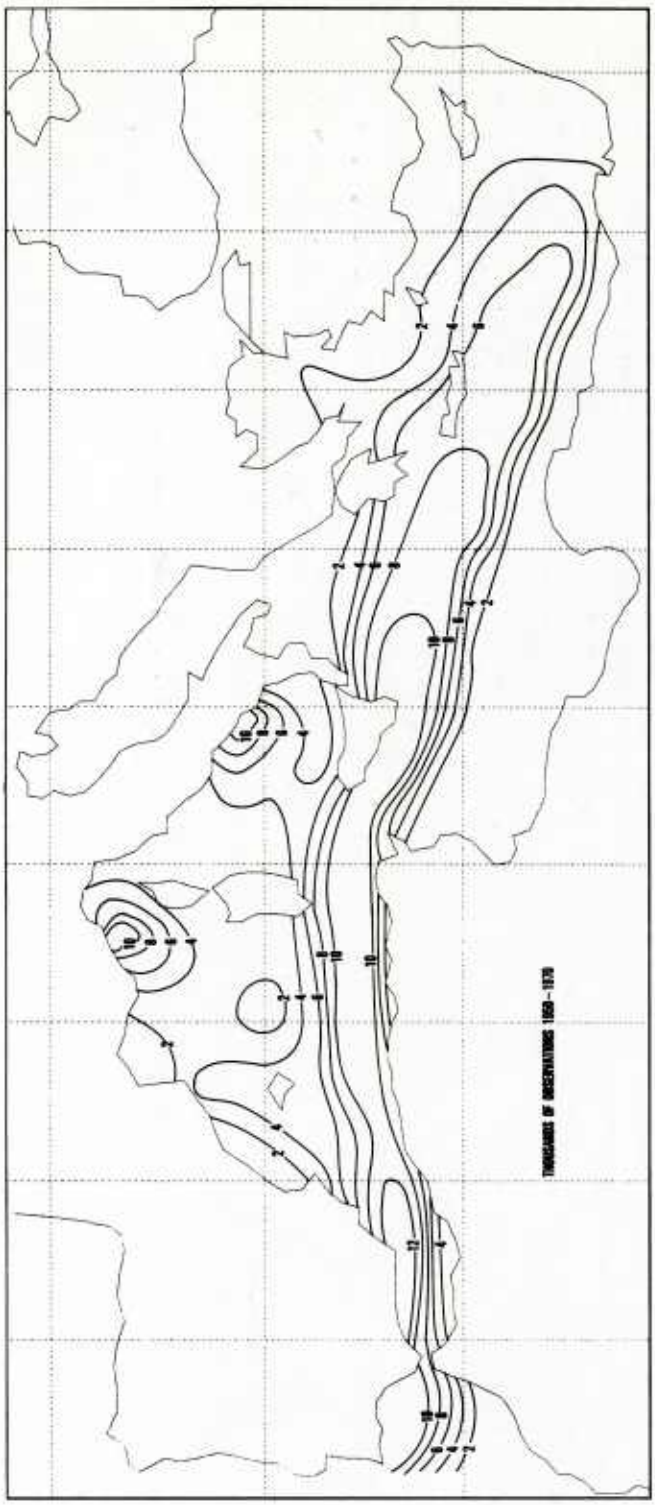

Figure 8. Contours of number of ship observations during the period 1950–1970

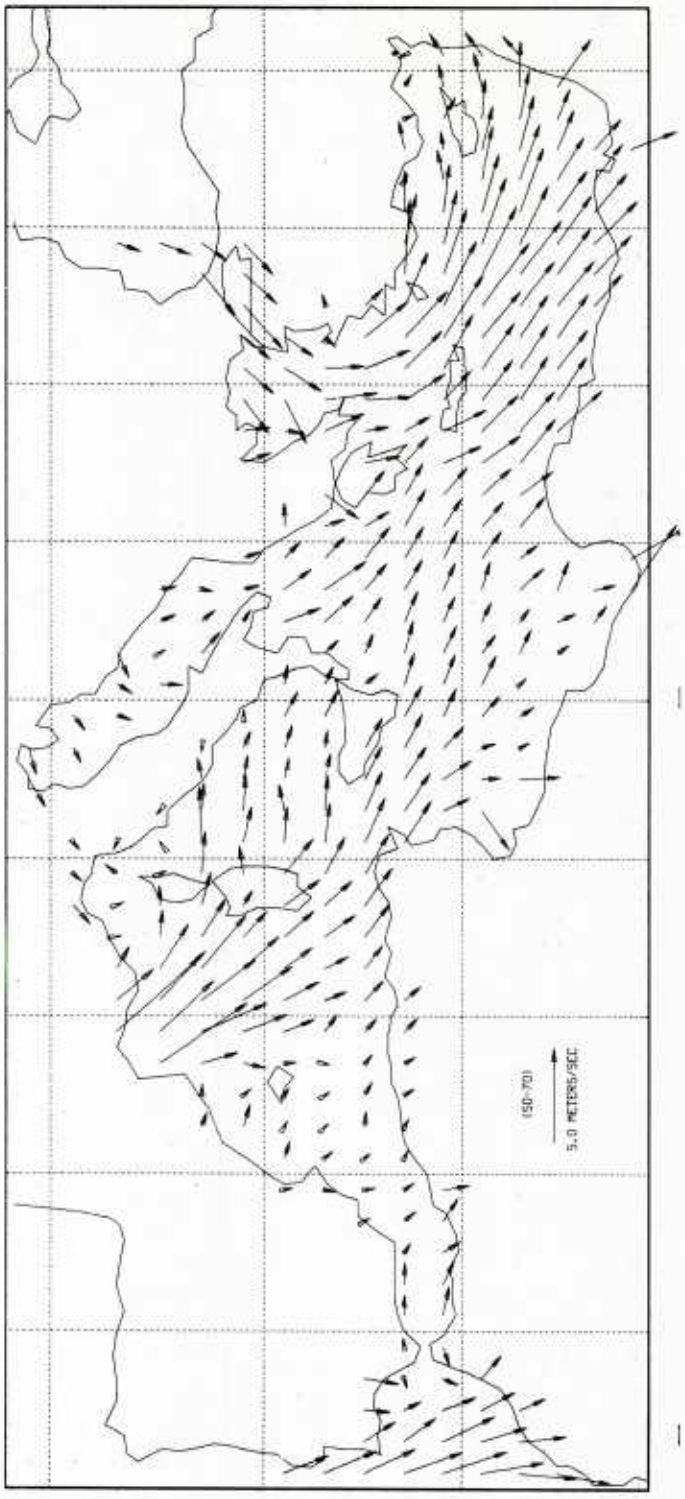

Figure 9. Annual average of the winds

wind field using ship observations from the period 1900-1940. Because their study uses comparable data and the same grid (1° x 1°), a comparison can easily be made between their annual average (Fig. 10) and that here. The results are very similar despite the differences in the number and time coverage of the observations. Most of the differences which appear in Figure 11, the present calculations minus Markgraf's data, are quite small with respect to the mean wind field. The larger deviations can easily be explained as a result of statistical uncertainty in the averages. Systematic differences, which can be seen along the southern coastlines of the Mediterranean, are probably too small to attribute to long-term secular change and may be the result of some of the errors discussed above.

The annual mean wind stress (Fig. 12) naturally exhibits patterns similar to that of the wind field. Its major feature is the strong southeastward stress in the western Mediterranean. Uniform eastward stresses in the Tyrhennian Sea contrast with westward stresses in the northern reaches of the Adriatic. Stress patterns in the eastern Mediterranean largely consist of eastward to southeastward stresses in the Ionian and Levantine basins, and southward stresses in the Aegean Sea. Magnitudes range from highs of nearly 3 dynes/cm^2 (0.3 pascal) in the northwestern Mediterranean to 0.5-1.0 dyne/cm^2 over much of the eastern basin.

The annual mean wind stress magnitude, contoured in Figure 13, has values that range from almost 3.0 dynes/cm^2 in the western Mediterranean to less than 0.8 dyne/cm^2 in large regions of the eastern basin and in the Alboran Sea/Baleric Sea region of the western basin. The Aegean Sea appears to be another area of relatively strong winds with magnitudes around 1.2 dynes/cm^2.

The vector curl of the wind stress is an important quantity which is readily calculated from the wind stress field. Figure 14 shows the curl calculated from the annual mean wind stress using centered differences to estimate derivatives. The curl's importance stems from its relation to the divergence of wind-driven surface currents and, hence, from a proportionality to vertical velocity at the base of the so-called Ekman layer (see Stommel, 1965). Given the short north-south extent of the Mediterranean and the relatively minor variations of the Coriolis parameter that this entails, the curl fields should be good indicators of vertical velocity with the rough conversion that curl of 1×10^{-8} dynes/cm^3 is equivalent to a vertical velocity of 10 cm/day. Two regions of significant curl appear in the figure: the Western Basin and the Aegean Sea. The magnitude of the mean annual vertical velocities that can be inferred from the stress curl to south of France is from 10 to 50 cm/day: upwelling in regions of positive curl and downwelling in regions of negative curl. Vertical velocities in the eastern Aegean are almost comparable.

Contours of mean annual wind stress variance (Fig. 15) show that wind stress in the western Mediterranean is highly variable as well as strong. The rest of the Mediterranean exhibits relatively uniform low variability even in regions where the winds are strong, such as the Aegean Sea.

On a seasonal basis, spring (March-May) stresses are characterized by moderate (2 dynes/cm^2) southwestward wind stress in the western Mediterranean and weak stress in the Aegean Sea and Ionian basin. The mean spring stress field, shown in Figure 16, also shows the eastward to southeastward stress of about 0.5 dyne/cm^2 that characterizes the Levantine basin throughout much of the year. Another point to note is the presence of weak southeastward stress along the Algerian coast.

Summertime stresses (Fig. 17) show weakening (1 dyne/cm^2) in the western Mediterranean but strengthening in the

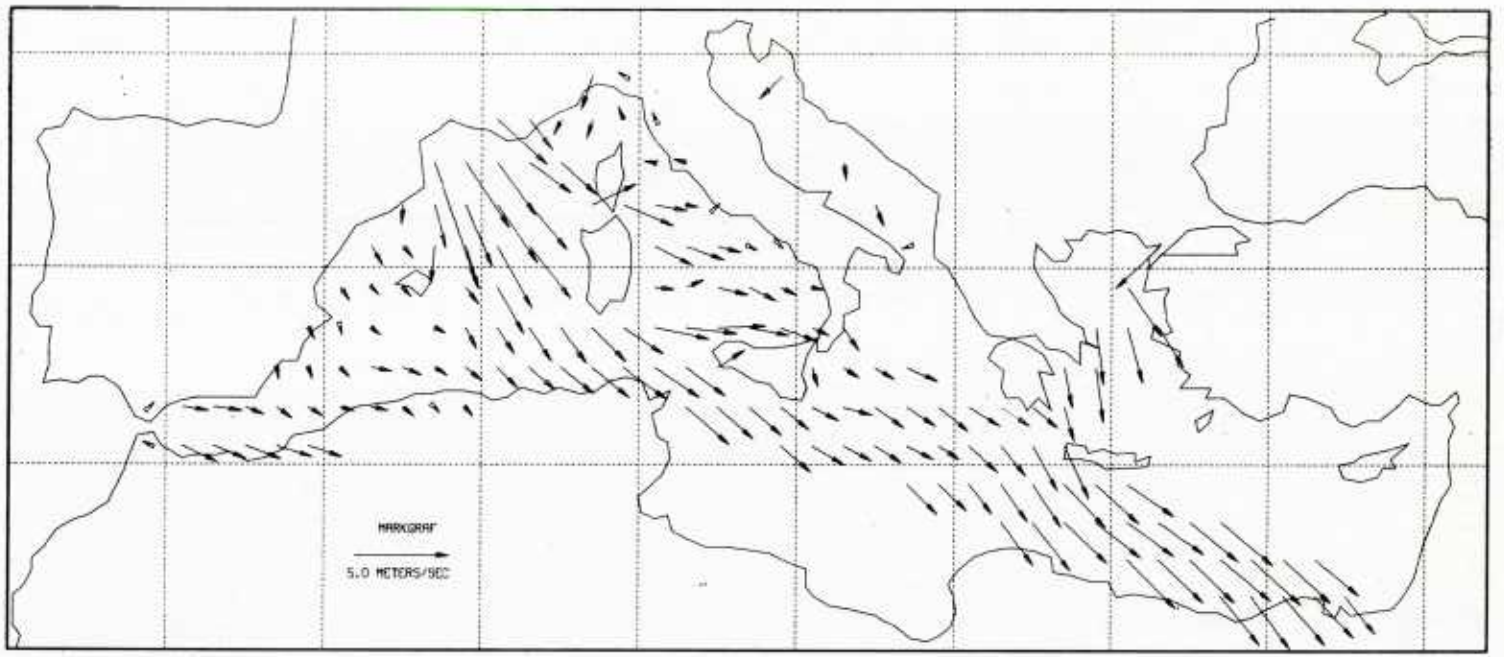

Figure 10. Markgraf and Niederschlag's annual wind average

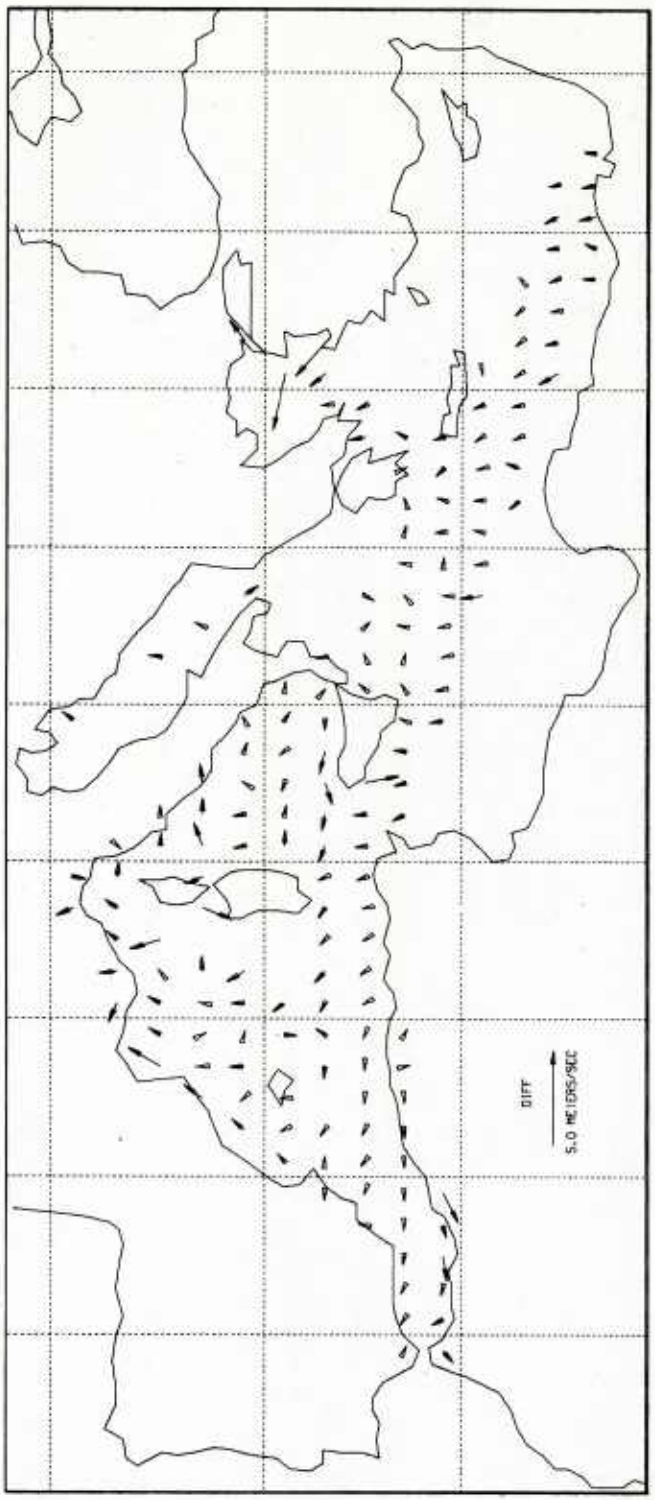

Figure 11. The difference between the winds of Figure 9 and Figure 10

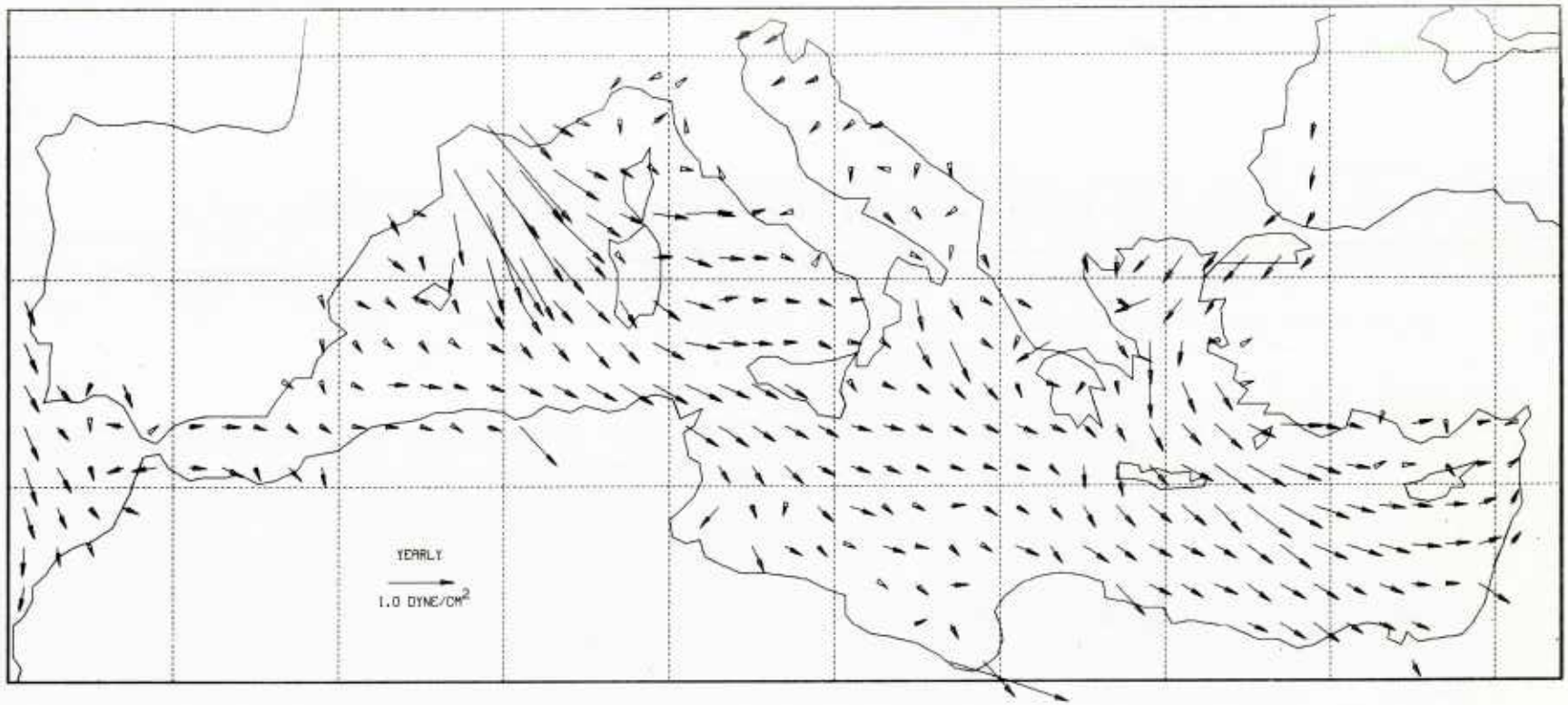

Figure 12. Unfiltered annual wind stress average for points with more than 100 ship observations

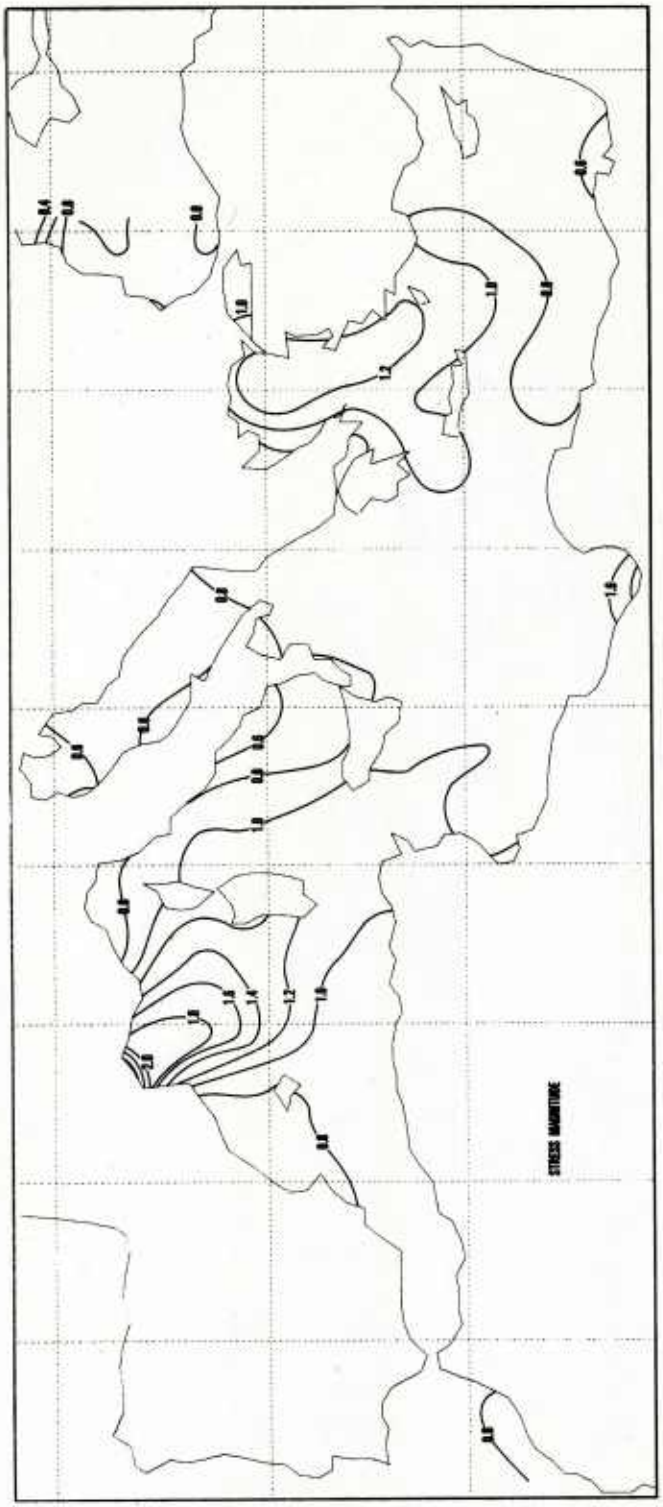

Figure 13. Contoured annual wind stress magnitude

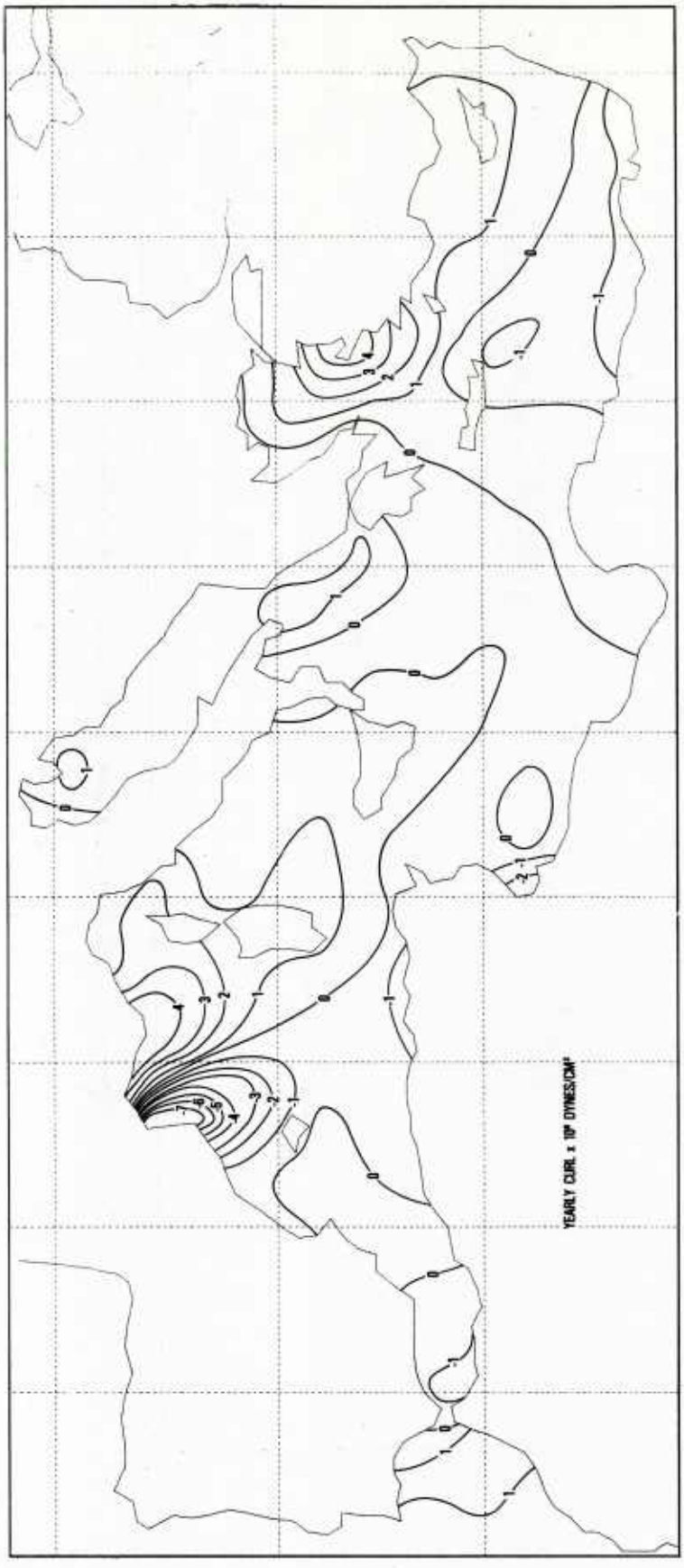

Figure 14. Contoured annual wind stress curl

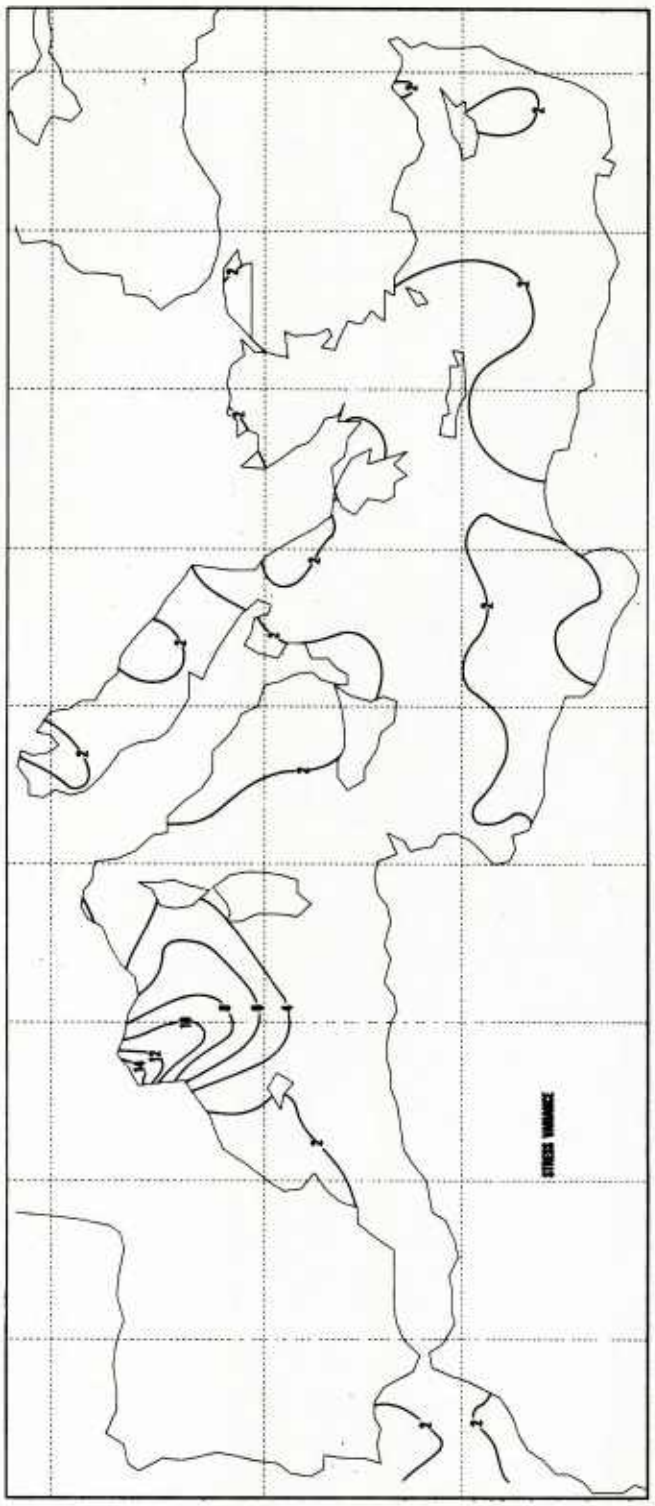

Figure 15. Contoured annual wind stress variance

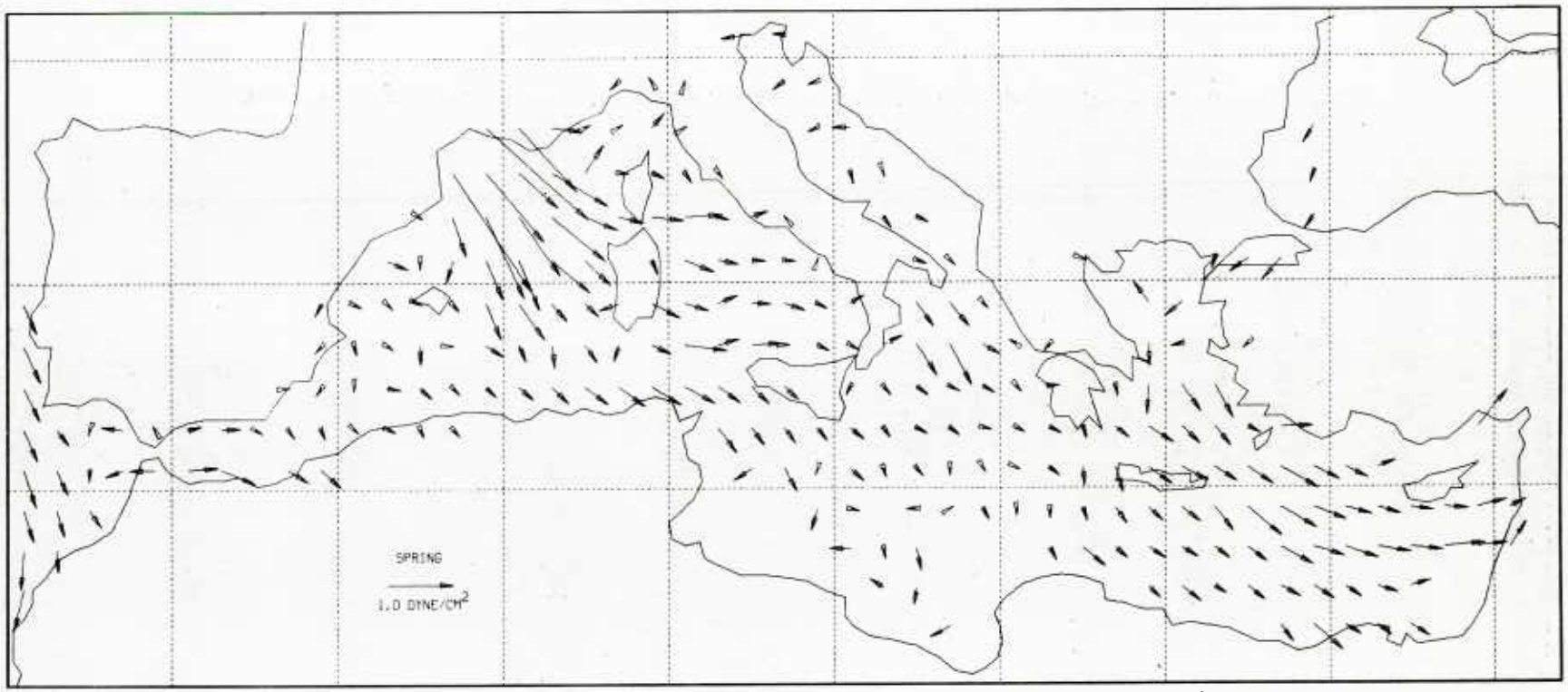

Figure 16. Spring wind stress average for points with more than 100 observations

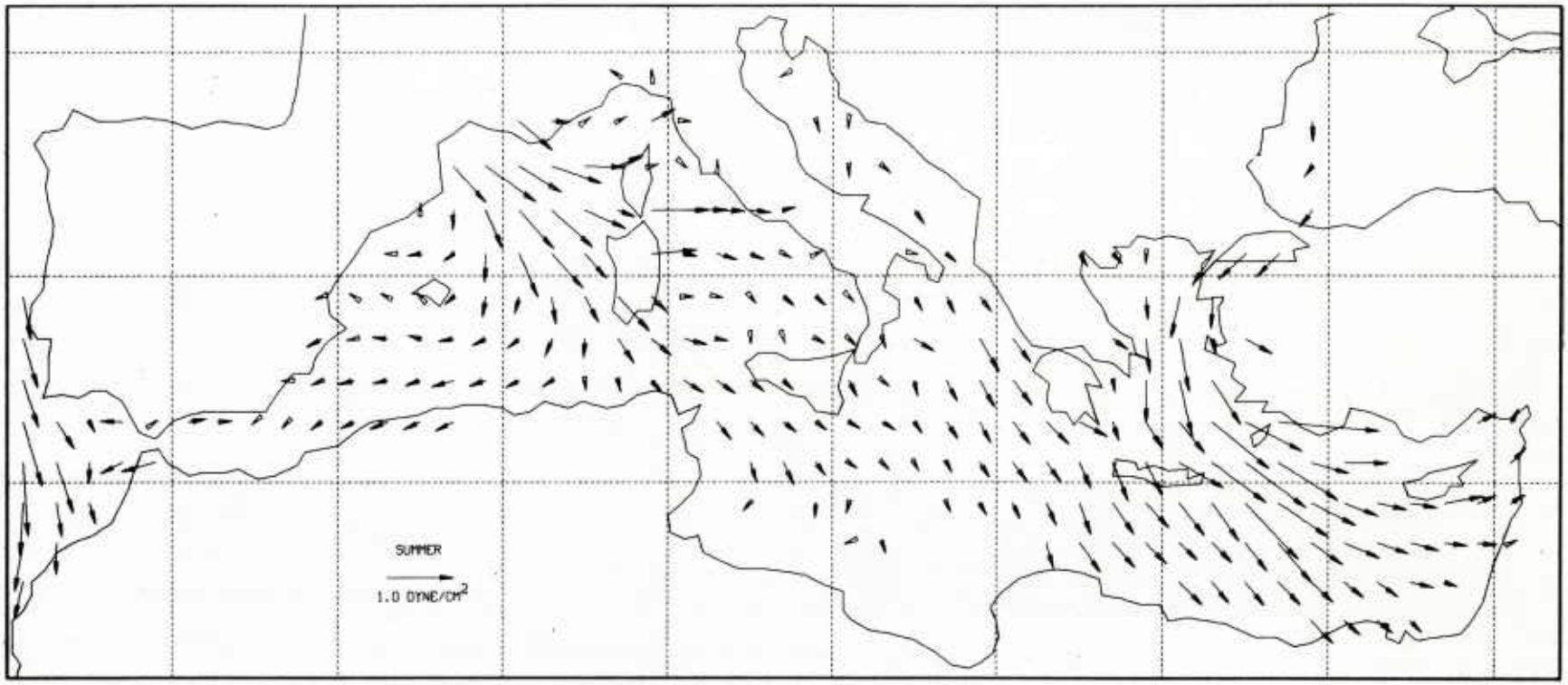

Figure 17. Summer wind stress average for points with more than 100 observations

Aegean Sea and Levantine basin. Stresses along the Algerian coast are southward to southwestward in contrast to the springtime stresses.

Autumn stress fields (Fig. 18) are very similar in strength and pattern to those of summer. Exceptions occur in the Ionian basin where southward stress shifts to weak eastward stress, and along the Algerian coast where stress reverses again to be come eastward.

Not surprisingly, winter stresses (Fig. 19) are generally strong over the entire Mediterranean, with the exception of the Aegean Sea where the stress is weak and appears to be controlled by a small cyclonic feature. The entire eastern Mediterranean is dominated by relatively strong (1 dyne/cm^2) eastward stress while the northwestern Mediterranean is dominated by 2-3 dynes/cm^2 southeastward stress. Several other regions also show significant increases in averaged stress. The northern reaches of the Adriatic Sea have strengthened stresses to the southwest and the Alboran Sea shows freshened stresses to the east. Because of its strength, the winter stresses are clearly the most important contribution to the annual average.

Monthly mean stresses are presented in an appendix. They exhibit the seasonal tendencies described above and show the transitions from season to season that justify the divisions. From these monthly means it is possible to assemble a time series of vector stresses for a particular region by averaging the stresses over the area for each month and plotting the twelve averages on a time axis. Figures 20-25 show the yearly cycle of wind stress for various Mediterranean basins.

These figures reiterate most of the points inferred from the seasonal stress plots. As noted above, the northwestern Mediterranean has the greatest stresses, with a maximum magnitude in December and a minimum in September. The direction of the stress is consistently around 145°.

By contrast, the Aegean Sea stress series shows a maximum in late summer or early autumn and a minimum during the winter months. The stresses in the Levantine basin are the most consistent throughout the year with magnitudes between 0.3 and 0.6 dyne/cm^2 and directions that range from 100° to 125°. The series in the southwestern Mediterranean (south of the Baleric Islands) clearly shows the stress reversal mentioned above.

An interesting additional calculation, which can be performed with the annual averages of winds and wind stresses, is the regression of the averaged stress on the averaged wind squared. Figures 26 and 27 show the scatter plots of these quantities for both the western and eastern portions of the Mediterranean and the least-squares regression lines. The slope of the regression lines can be related to a drag coefficient for use with averaged winds. These slopes indicate a drag coefficient of 5.6×10^{-3} for the western basin and 2.3×10^{-3} for the eastern basin. The difference between the two drag coefficients is indicative of the difference in wind variability for the eastern and western basins of the Mediterranean. The difference also justifies the calculation and averaging of individual stresses, since a priori knowledge of drag coefficients for averaged winds was not available. The conclusion is that if the averaged winds had been used with a typical drag coefficient of 1.5×10^{-3}, the stresses would have been severely underestimated.

IV. Discussion

A number of the wind systems that cause the wind stress patterns noted are so persistent that they have been given names: Mistral, Bora, Scirocco, Levanter, Vendaval, Libeccio, and Etesians are names of several regional wind systems in the Mediterranean. Only the strongest of these systems (the Mistral, the Etesians, and the Bora) were detectable in the climatological averages, however.

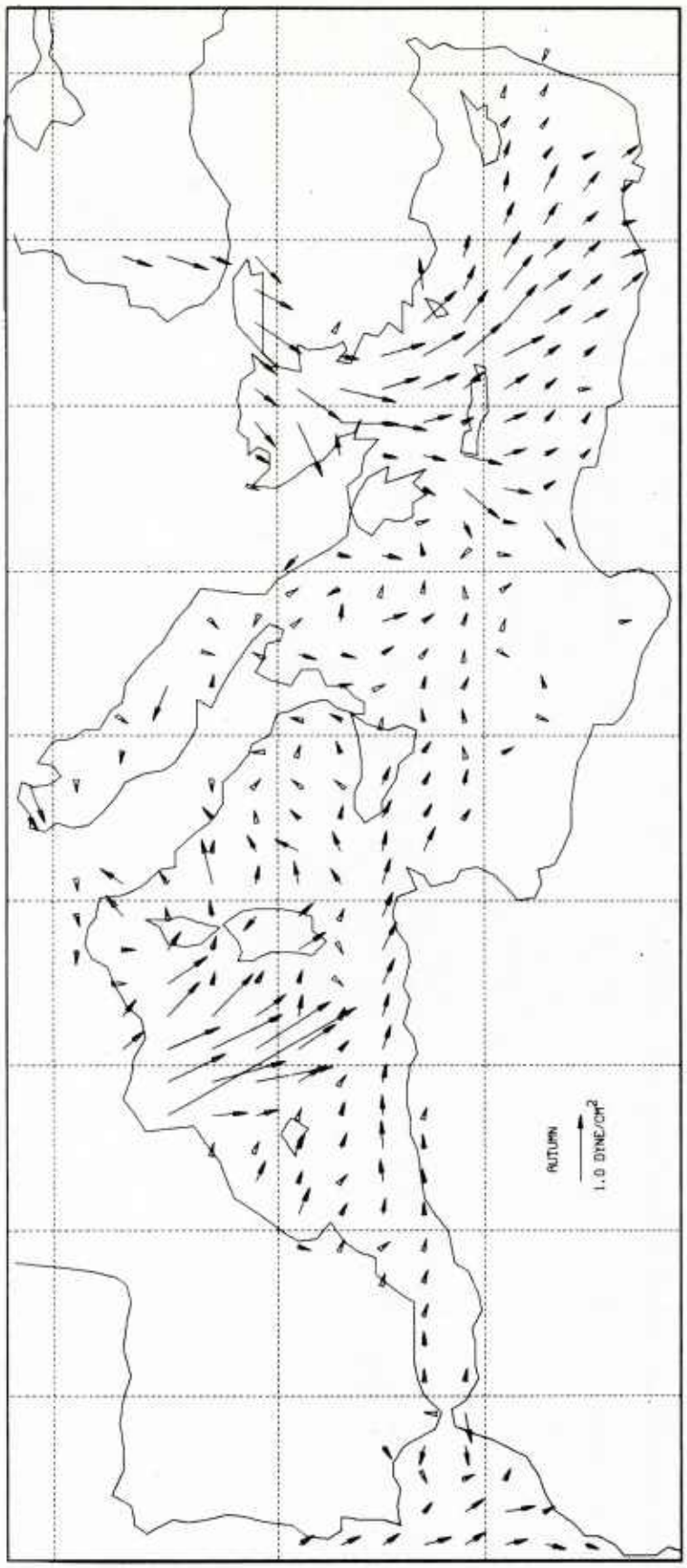

Figure 18. Autumn wind stress average for points with more than 100 observations

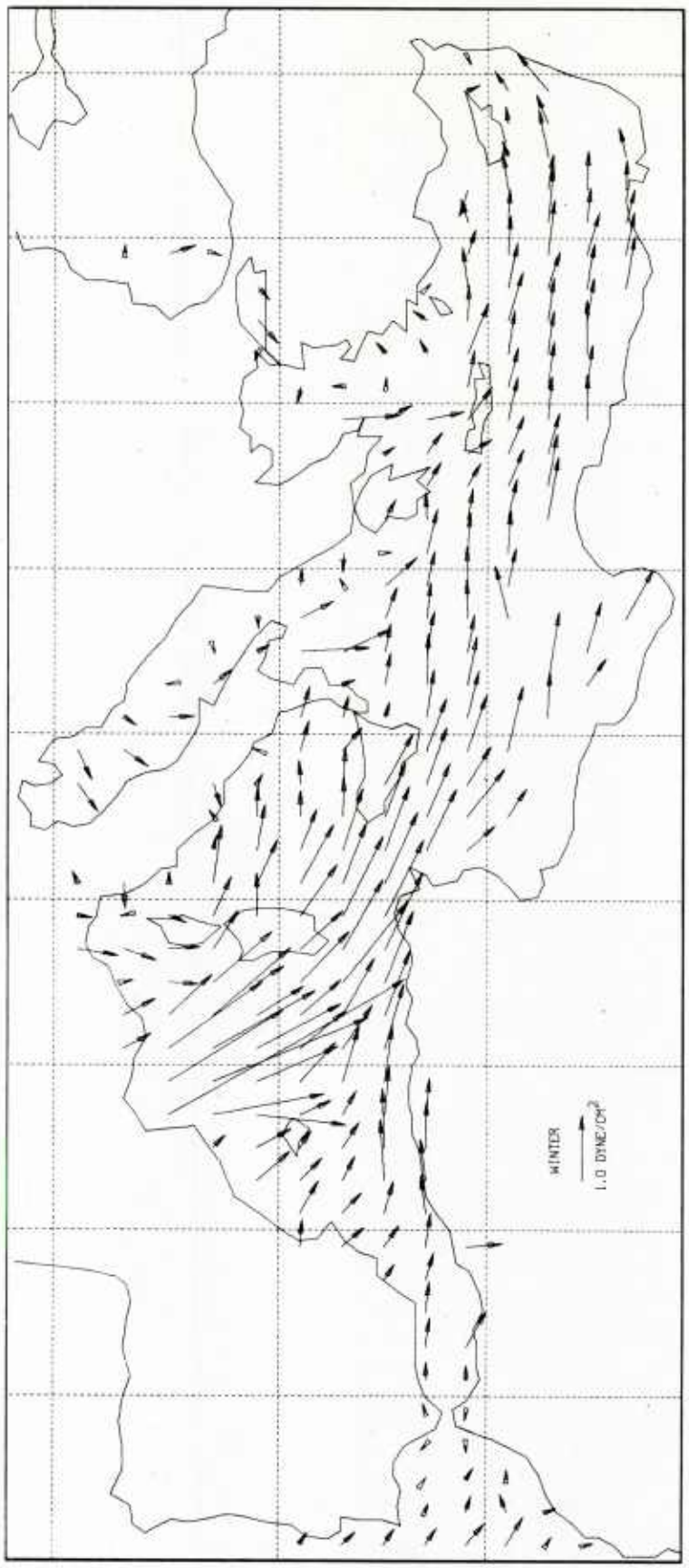

Figure 19. Winter wind stress average for points with more than 100 observations

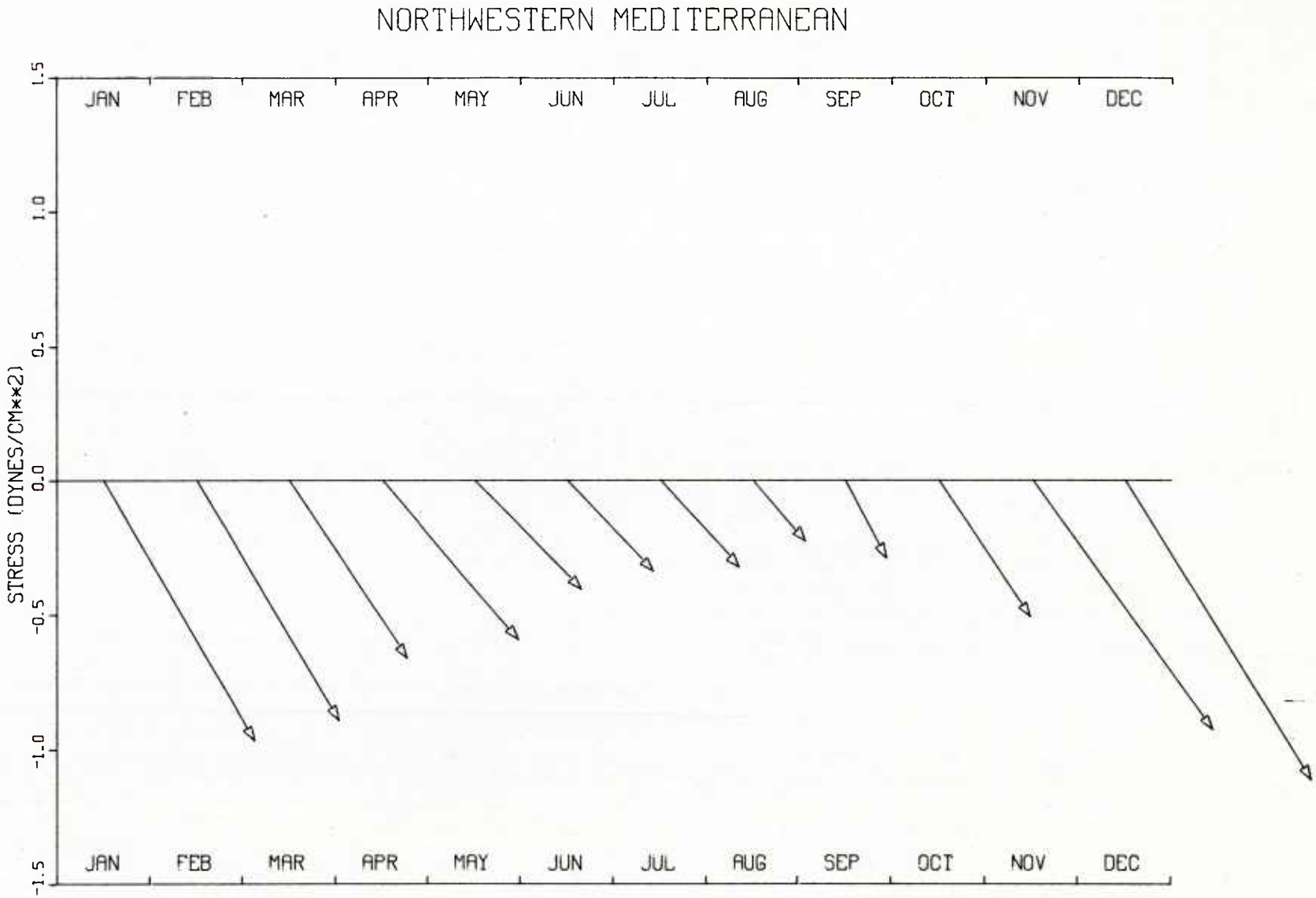

Figure 20. Year-long cycle of stresses in the northwestern Mediterranean

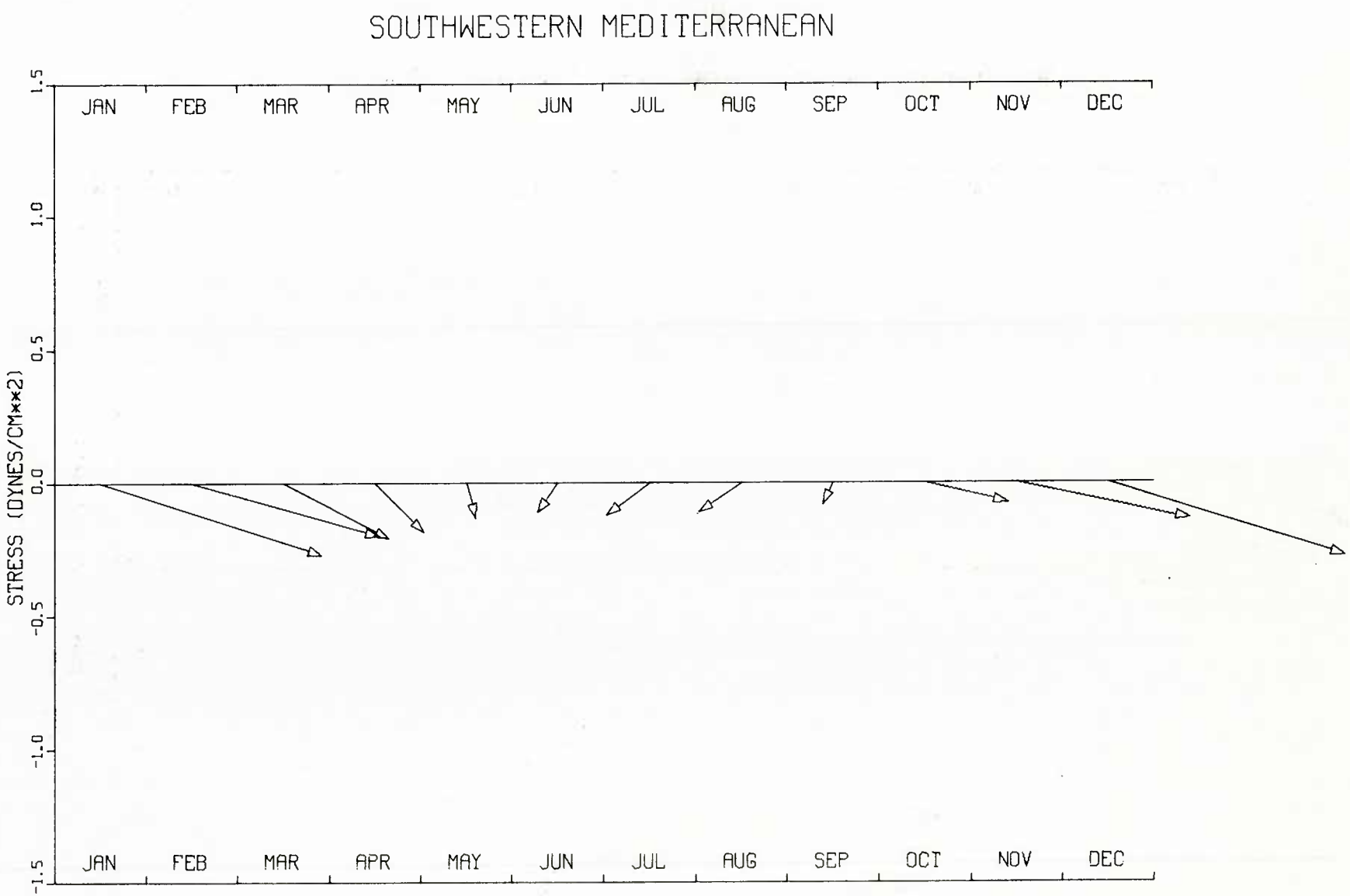

Figure 21. Year-long cycle of stresses in the southwestern Mediterranean

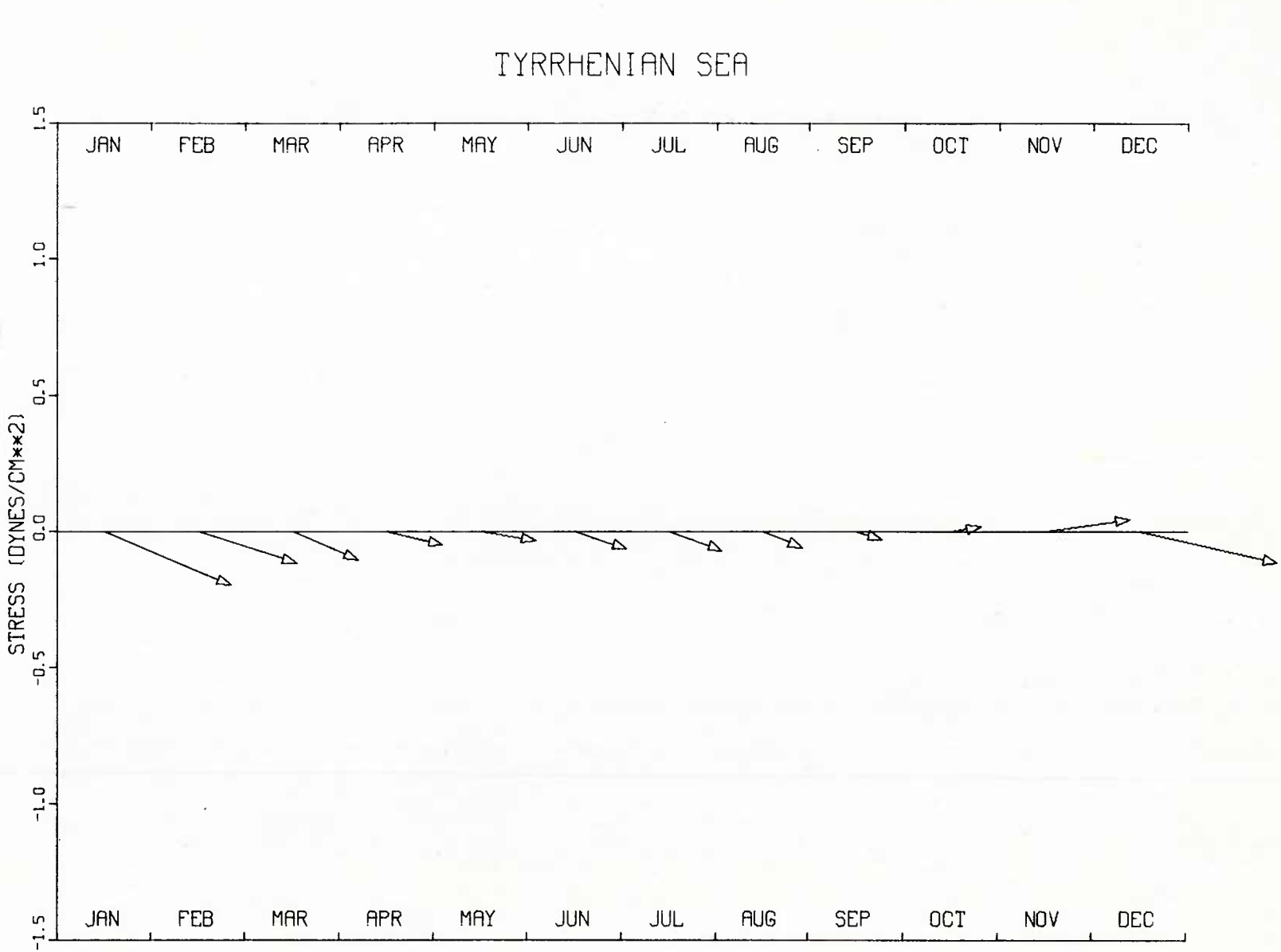

Figure 22. Year-long cycle of stresses in the Tyrhennian Sea

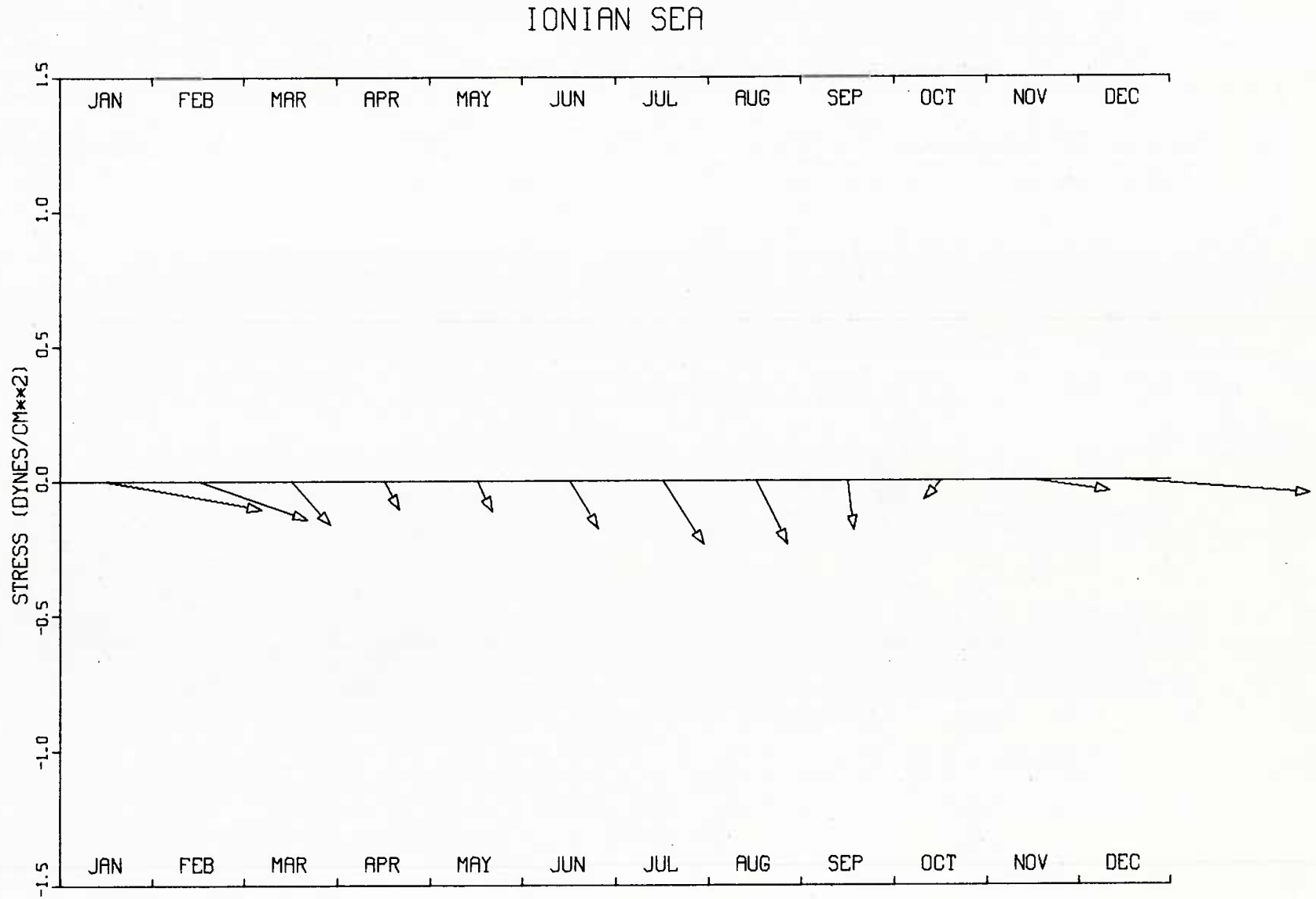

Figure 23. Year-long cycle of stresses in the Ionian Sea

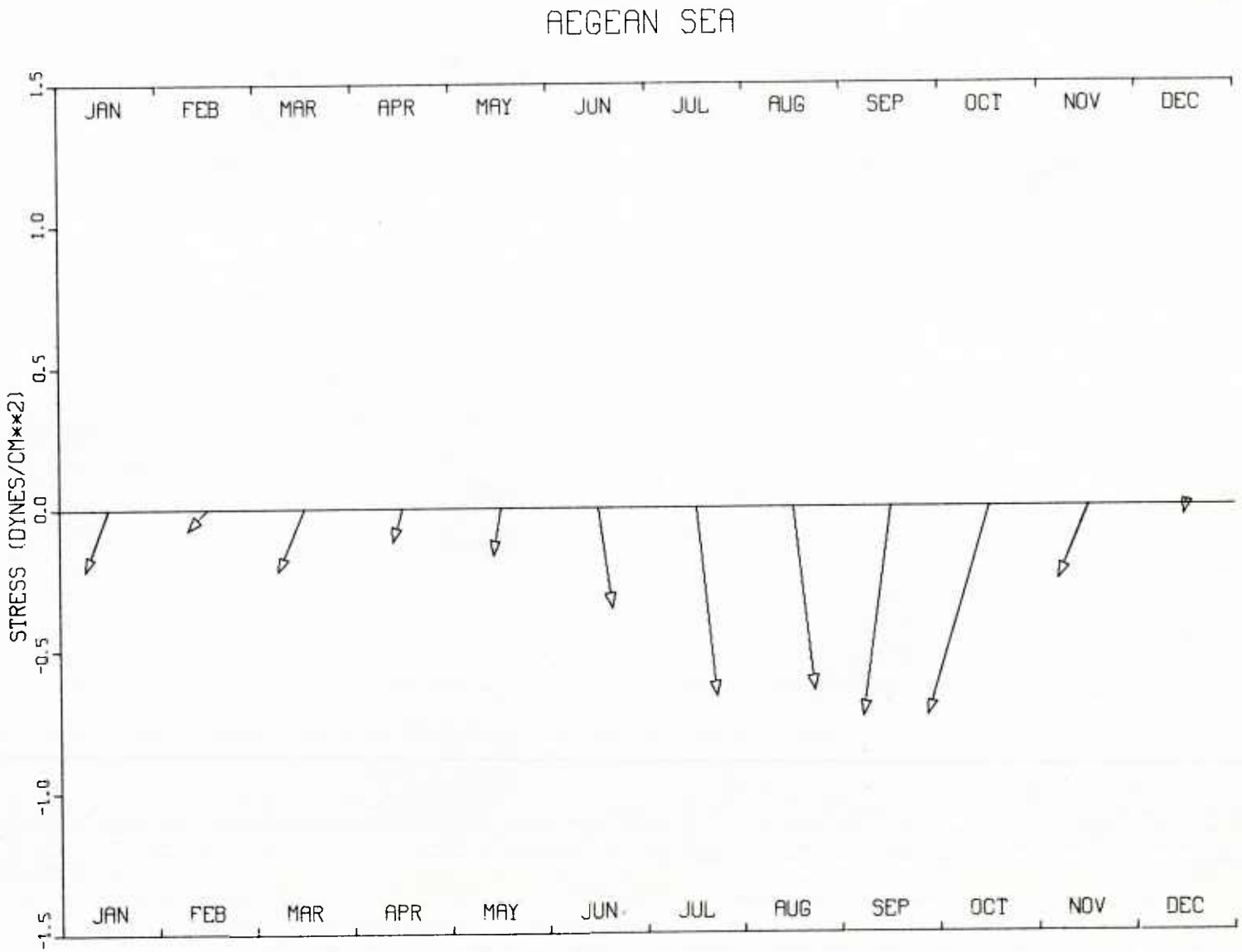

Figure 24. Year-long cycle of stresses in the Aegean Sea

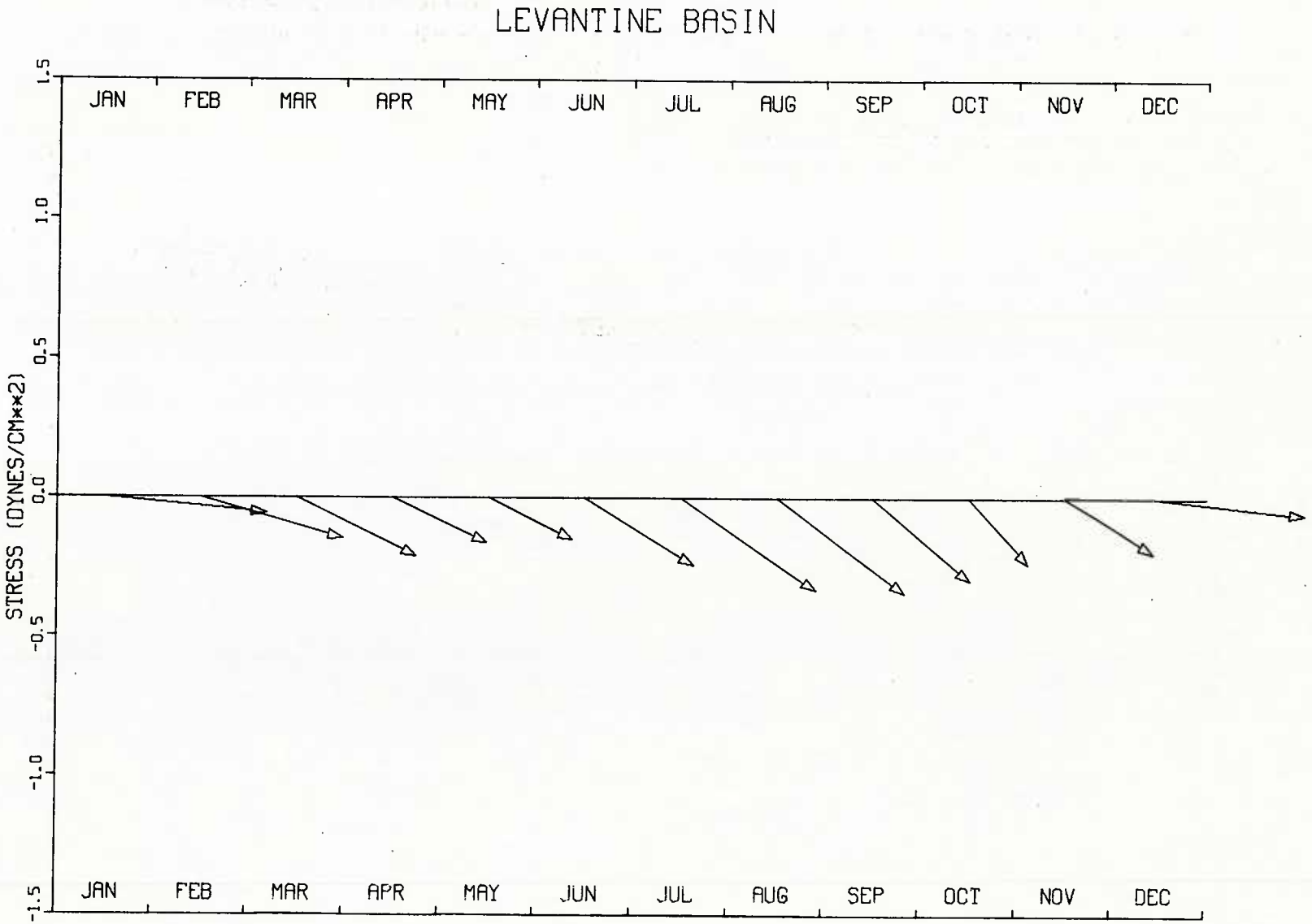

Figure 25. Year-long cycle of stresses in the eastern Mediterranean

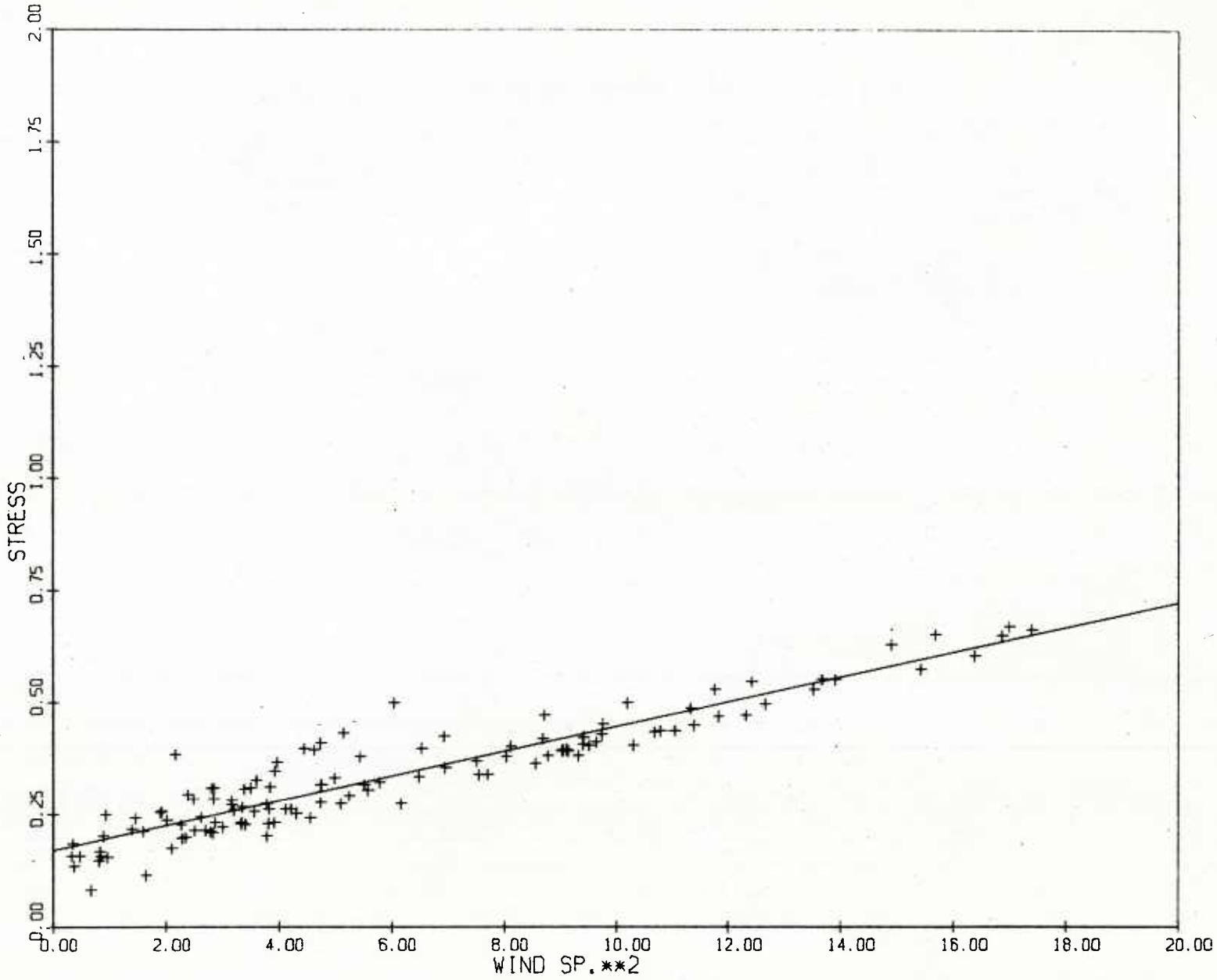

Figure 26. Scatter plot of average stress (dynes/cm^2) vs. average wind speed (m/sec)^2 for eastern Mediterranean

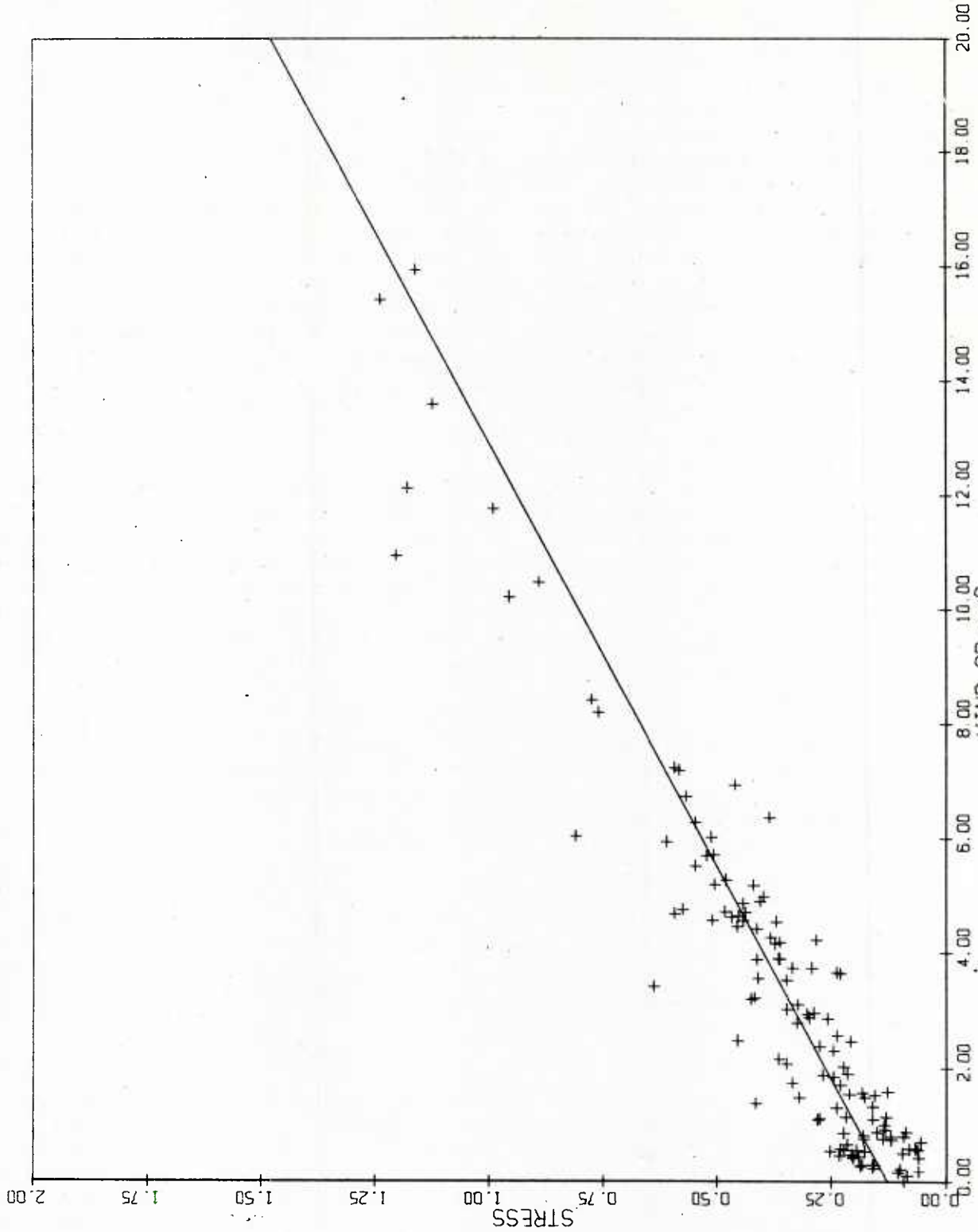

Figure 27. Scatter plot of average stress (dynes/cm^2) vs. average wind speed (m/sec)^2 for western Mediterranean

A. The Mistral

The Mistral is the intense northwesterly wind that appears during all seasons in the western basin of the Mediterranean. It blows down Rhone River valley through the gap between the Pyrenees and the Alps (the Garronne-Carcassone gap). It is a cold, dry, and very persistent wind that meets the Mediterranean at the Golfe du Lion and is responsible for the large southeastward stresses in the climatological averages. The heat loss which results as the Mistral sweeps across the northwestern Mediterranean during the winter is thought to be responsible for the large regions of convective overturning that have been observed in the area (MEDOC Group, 1970). The Mistral is also responsible for the large values of wind-stress curl that have been calculated from the stress averages. Its narrow, jet-like profile and strong, persistent stress magnitudes result in large gradients across the axis of the wind and, hence, in large wind-stress curls; negative curl to the right of the Mistral's axis and positive curl to the left of the axis looking downwind.

The vertical motion that results from the divergence of horizontal currents in the Ekman layer is substantial for oceanic conditions. Vertical velocities of up to 70 meters/day are possible, given the magnitude of the curl computed in the Golfe du Lion region. Since these figures are long-term averages, individual months or seasons are liable to exhibit even larger vertical movements. The effects on the mean circulation in the region should certainly be substantial enough to observe with classical oceanographic surveys.

Hydrographic surveys of the Northwestern Mediterranean do show the presence of a large cyclonic gyre centered approximately at 42N and 5E (Ovchinnikov, 1966). This circulation feature is a reasonable consequence of the positive curl and upward motion that is inferred from the wind stress calculations.

Direct measurements of vertical velocity by Voorhis and Webb (1970) during the MEDOC experiment indicate that large (2 cm/sec) upward velocities do exist in the region and are persistent over periods of several days. Calculations of vertical velocities by Seung (1980) also show substantial upward movement on monthly time scales. More significantly, Swallow and Canton (1973) suggest that the gyre plays an important role in the initial or preconditioning stages of bottom water formation by bringing the salty intermediate water close to the surface. The possibility that the Mistral is responsible for preparing the northwestern Mediterranean for bottom water formation as well as for the actual cooling of the surface water is an interesting topic for future study.

Corroborating evidence for the large downward velocities, which should occur to the west of the Mistral's axis, has not been found. Hydrographic surveys do not seem to show any indication of an anticyclonic gyre. Measurements that indicate downward bursts of water during the intense cooling of winter are clearly irrelevant to the Ekman layer arguments advanced here, but it should be noted that the direct measurements cited are all to the east of the region of negative wind-stress curl.

B. The Etesians

In the eastern Mediterranean the dominant winds are the Etesians (Greek) or Meltems (Turkish). These winds are funneled on to the Aegean Sea through the gap that exists between the mountains of the Balkans and the mountains of Anatolia--i.e., along the Rosporos and Dardanelles, and the Maramara Sea. The Etesians are also northerly winds, but are strongest in the late summer or early autumn. The region of positive wind-stress curl which hugs the Turkish coast is another area that has been indicated in the formation of subsurface water masses in the Mediterranean (Wust, 1961). There seems to be no evidence, however, that the Etesian wind system

has any effect on the hydrography of the area or the process of cooling.

C. The Bora

The last of the Mediterranean wind systems to be evident in the 20-year averages is the Bora. The Bora is another wind that is directed by the topography of the region--in this case, the Trieste gap at the northern end of the Adriatic Sea. This break between the European and Dinaric Alps directs a westward flow over the northern Adriatic. The Bora is a strong but infrequent winter wind; consequently, it appears only as a slightly larger westward stress in the winter averages.

V. Summary

Twenty-year mean winds and wind stresses have been calculated from the ship observation reports of the National Climatic Center. The winds, stresses, and derived quantitites are organized into monthly, seasonal, and annual mean fields with one degree resolution. Smoothed versions of all fields were also prepared. Estimates of the wind stress were obtained using an aerodynamic drag law to calculated stresses from individual ship reports. The stress estimates were then averaged on the one degree squares for each month for the 20-year period.

The average wind and stress field show the major wind systems of the Mediterranean Sea. Of these systems, the Mistral and Etesian winds are the most obvious. The Mistral is of particular interest due to its influence on bottom water formation and wind driven circulation in the western Mediterranean.

VI. References

Bunker, A. F. (1976). Computations of Surface Energy Flux and Annual Air-Sea Interaction Cycles of the North Atlantic Ocean. Mon. Wea. Rev. v. 109, p. 1122-1140.

Bunker, A.F. and R.A. Goldsmith (1979). Archived Time-Series of Atlantic Ocean Meteorological Variables and Surface Fluxes. Woods Hole Oceanographic Institute Technical Report WHOI-79-3, 28 p.

Garratt, J. R. (1977). Review of Drag Coefficients Over Oceans and Continents. Mon. Wea. Rev., v. 105, p. 915-929.

Hastenrath, S. and P. Lamb (1978). Heat Budget Atlas of the Tropical Atlantic and Eastern Pacific Oceans. Univ. of Wisconsin Press, Madison, 90 p.

Hellerman, S. (1965). Computations of Wind Stress Fields Over the Atlantic Ocean. Mon. Wea. Rev., v. 93, p. 239-244.

Kondo, J. (1975). Air-Sea Bulk Transfer Coefficients in Diabatic Conditions. Boundary-Layer Met., v. 9, p. 91-112.

Large, W. G. and S. Pond (1981). Open Ocean Momentum Flux Measurements in Moderate to Strong Winds. J. Phys. Oceanog., v. 11, p. 324-336.

Markgraf, H. and N. Niederschlag (1961). Klimatologie Des Mittelmeeres, Teil 1, Windkarten. Deutscher Wetterdienst, Hamburg.

MEDOC Group (1970). Observation of Formation of Deep Water in the Mediterranean Sea, 1969. Nature, v. 227, p. 1037-1040.

Ovchinnikov, I. M. (1966). Circulation in the Surface and Intermediate Layers of the Mediterranean. Oceanology, v. 6, p. 48-59.

Saunders, P. M. (1976). On the Uncertainty of Wind Stress Calculations. J. Mar. Res., v. 34, p. 155-160.

Seung, Y. H. (1980). Low-Frequency Vertical Motions in the Medoc Area of Deep Water Formation. Oceanol. Acta., v. 3, p. 441-447.

Stommell, H. (1965). The Gulf Stream. Univ. of California Press, Berkely, 249 p.

Swallow, J. C. and G. F. Canton (1973). The Preconditioning Phase of MEDOC 1969--I. Observations. Deep-Sea Res., v. 20, p. 429-448.

Voorhis, A. D. and D. C. Webb (1970). Large Vertical Currents Observed in a Winter Sinking Region of the Northwestern Mediterranean. Cah. Oceanog., v. 22, p. 571-580.

Weare, B. C. and P. T. Strub (1981). The Significance of Sampling Biases on Calculated Monthly Mean Oceanic Surface Heat Fluxes. Tellus, v. 33, p. 211-224.

Wust, G. (1961). On the Vertical Circulation of the Mediterranean Sea. J. Geophys. Res., v. 66, p. 3261-3271.

Appendix: Monthly Mean Stresses

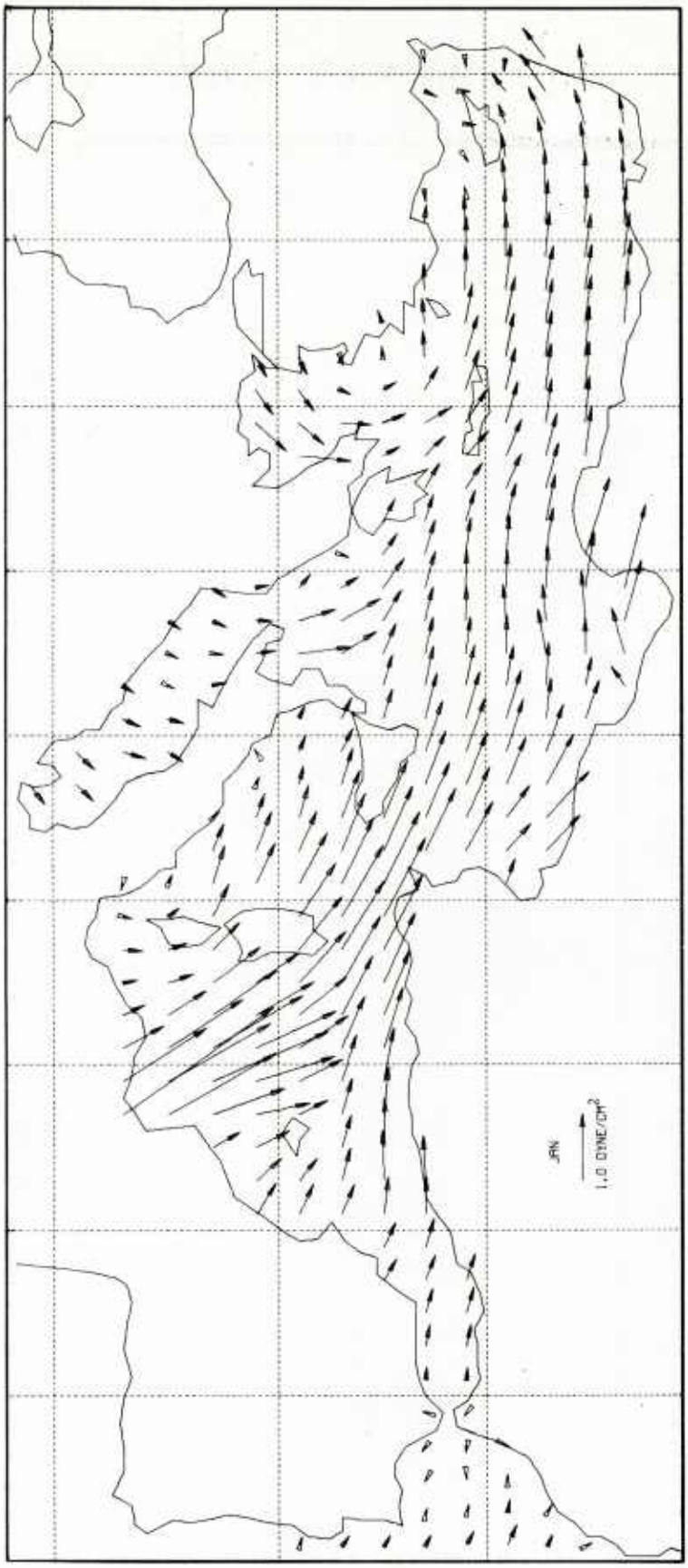

Figure A1. January wind stress (filtered)

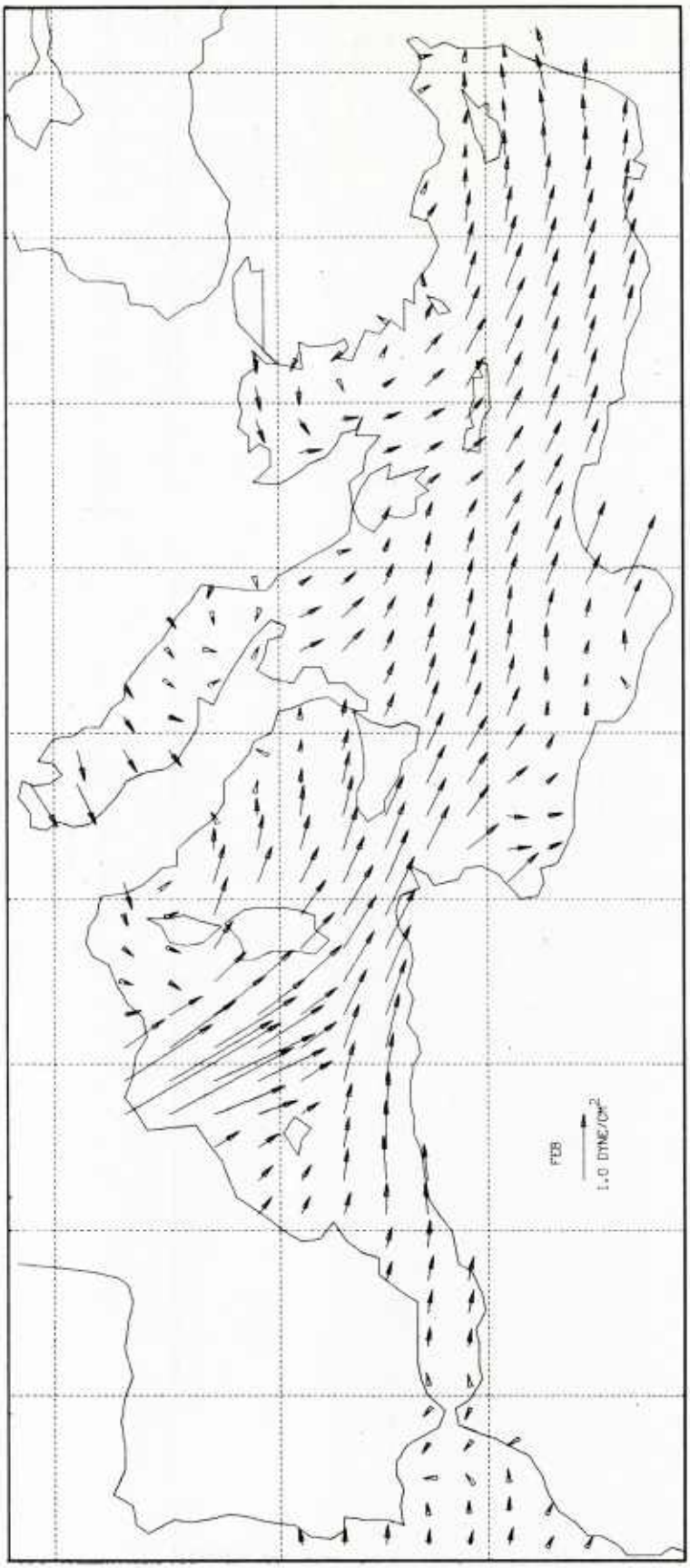

Figure A2. February wind stress (filtered)

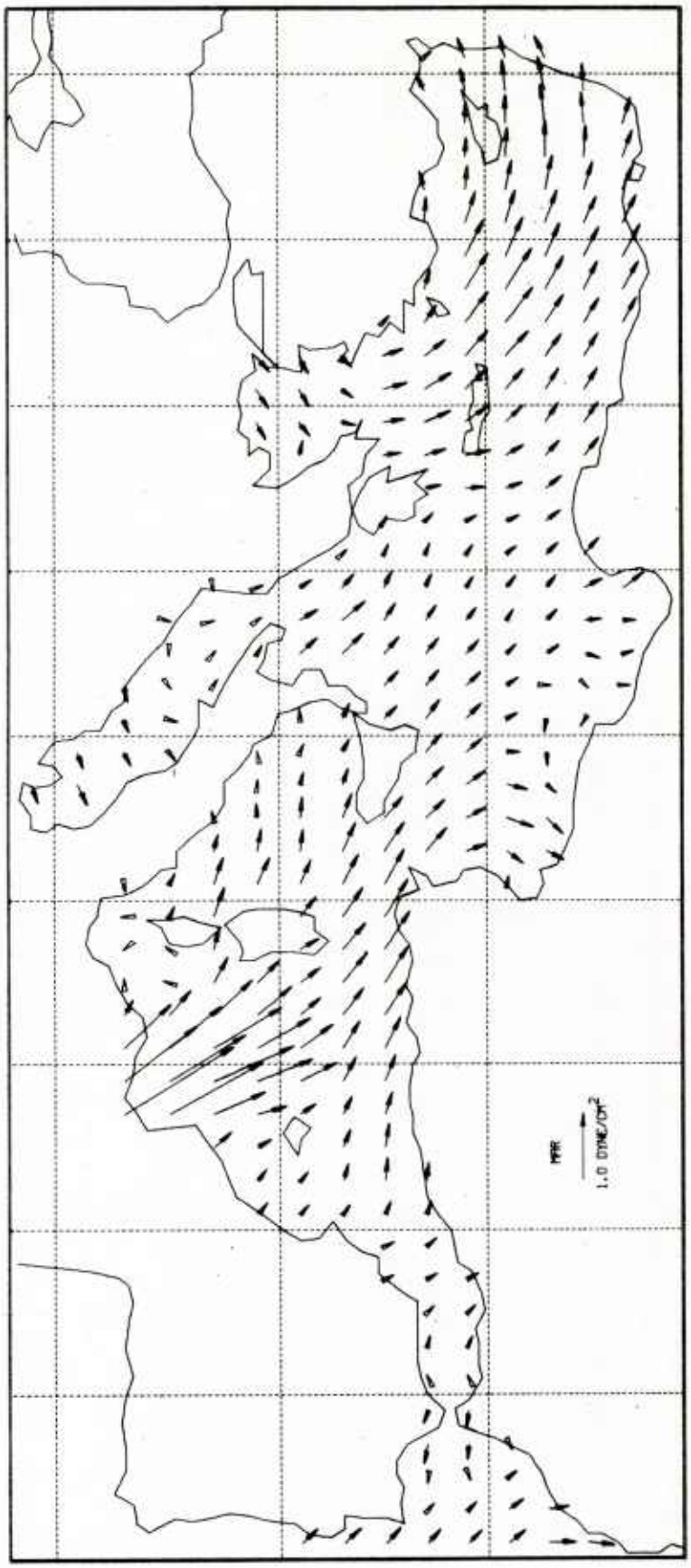

Figure A3. March wind stress (filtered)

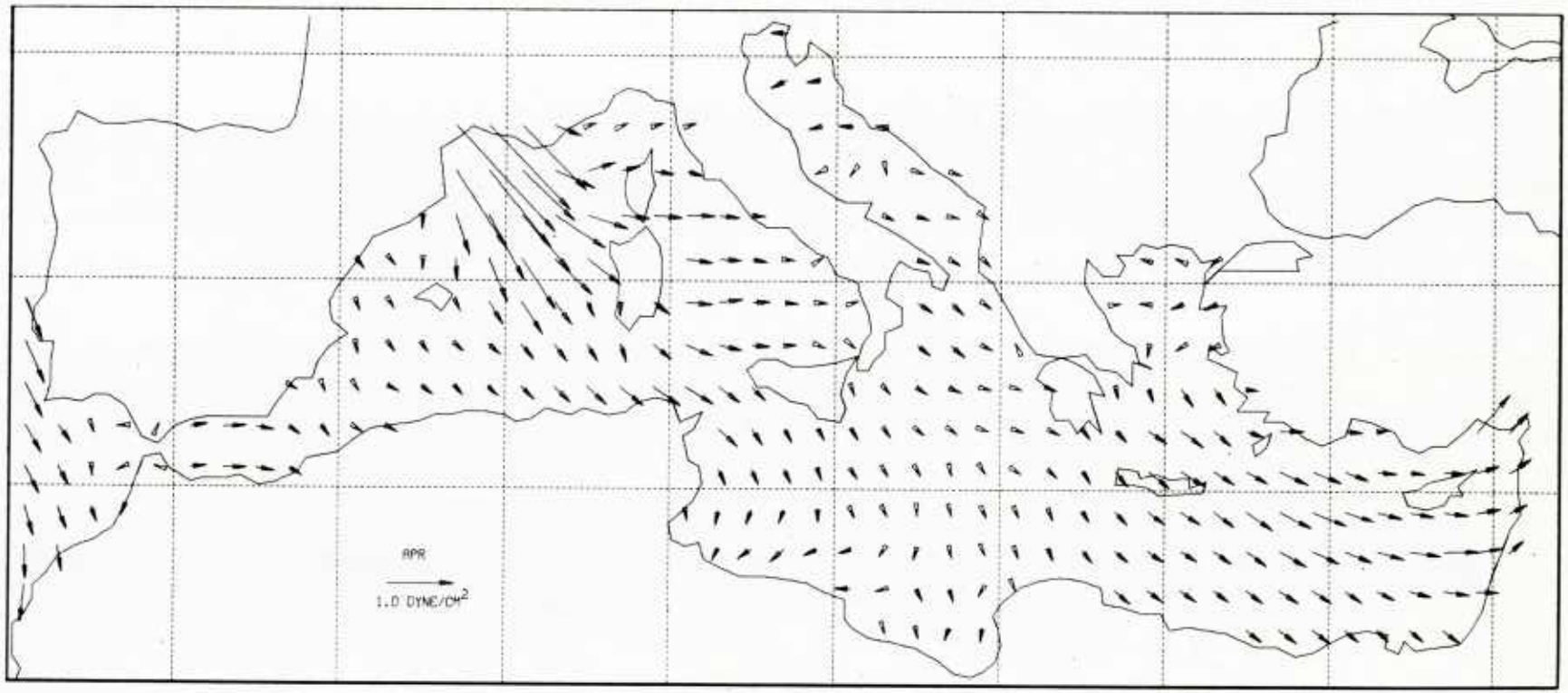

Figure A4. April wind stress (filtered)

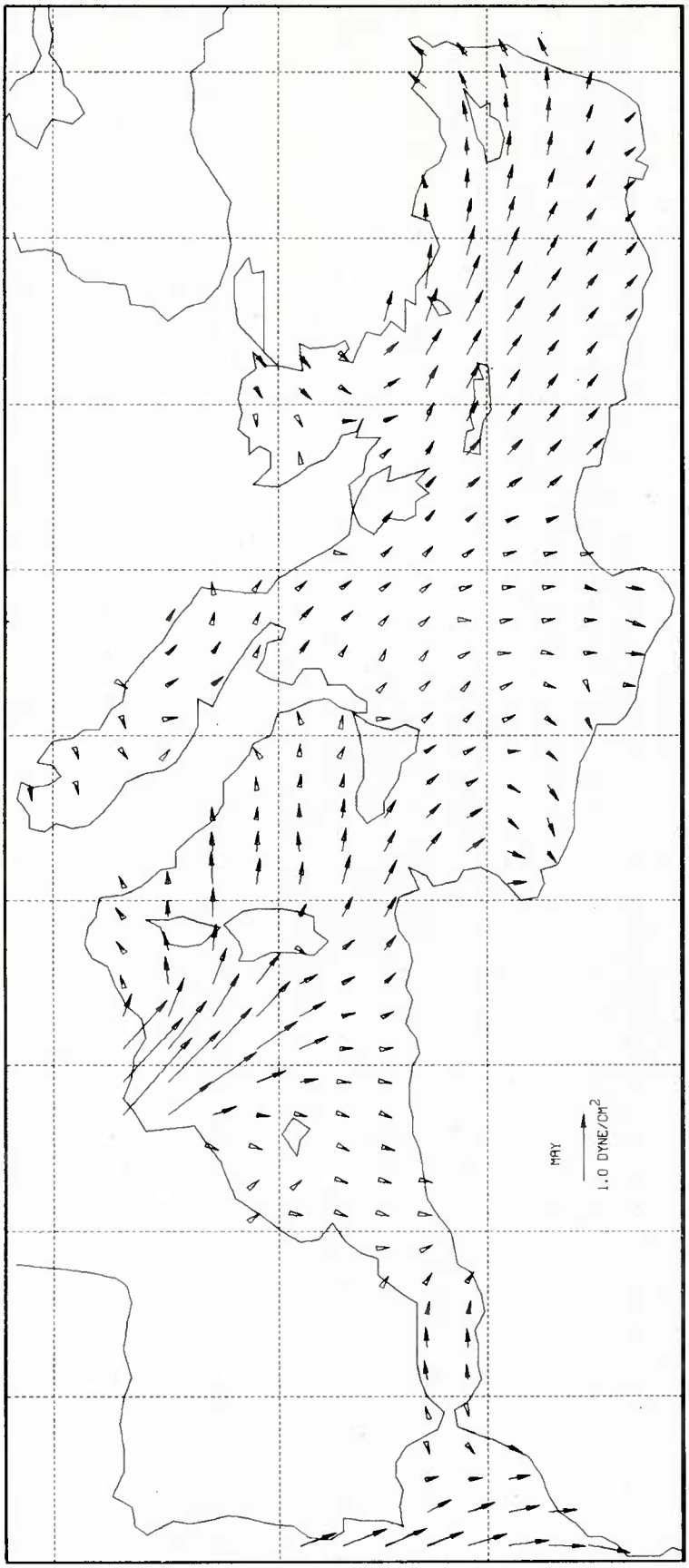

Figure A5. May wind stress (filtered)

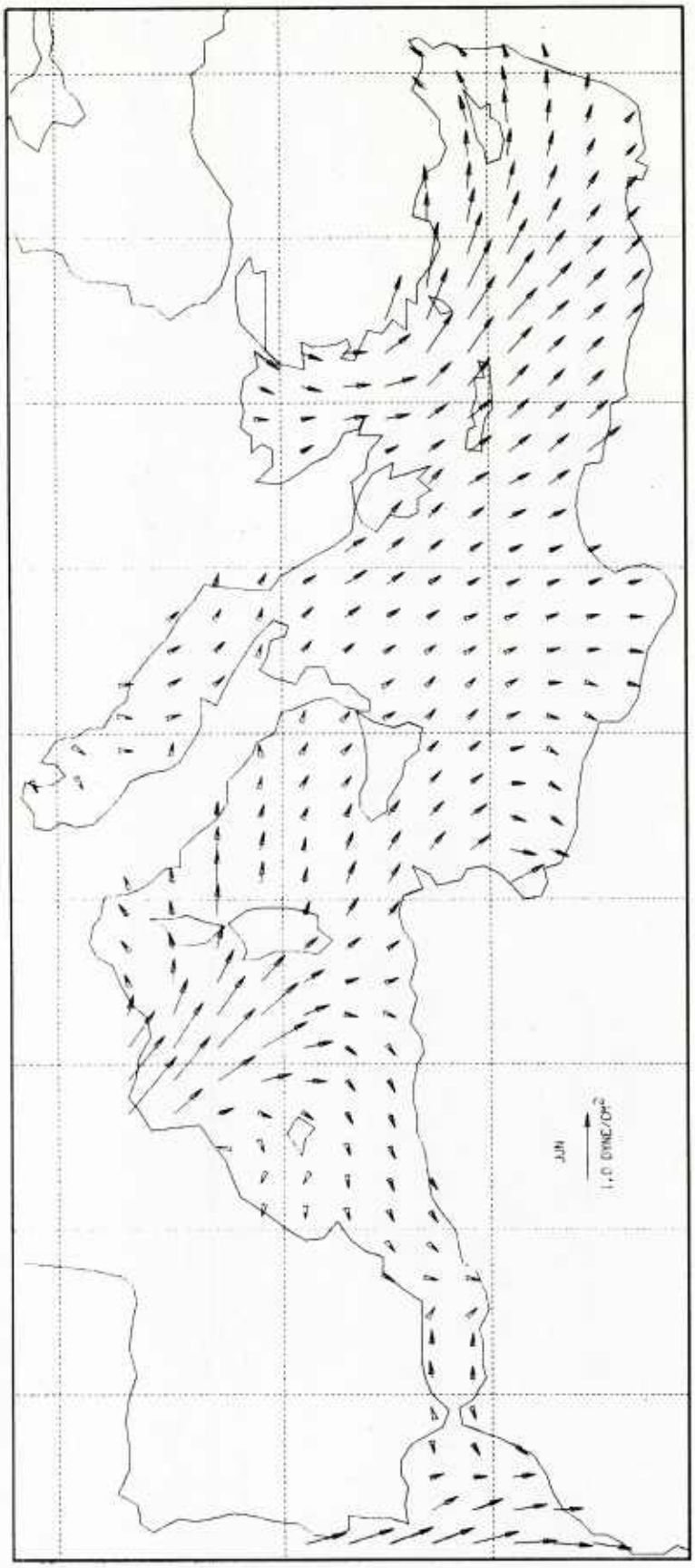

Figure A6. June wind stress (filtered)

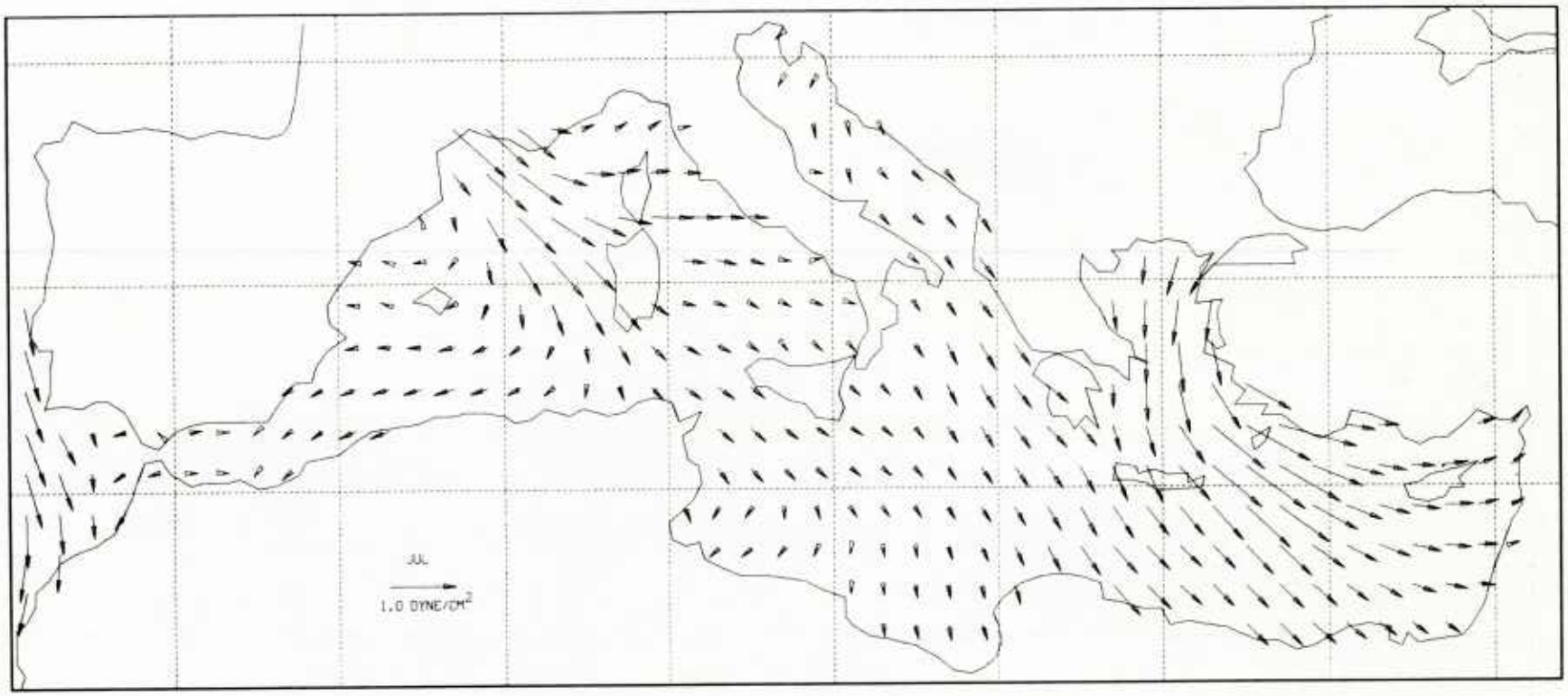

Figure A7. July wind stress (filtered)

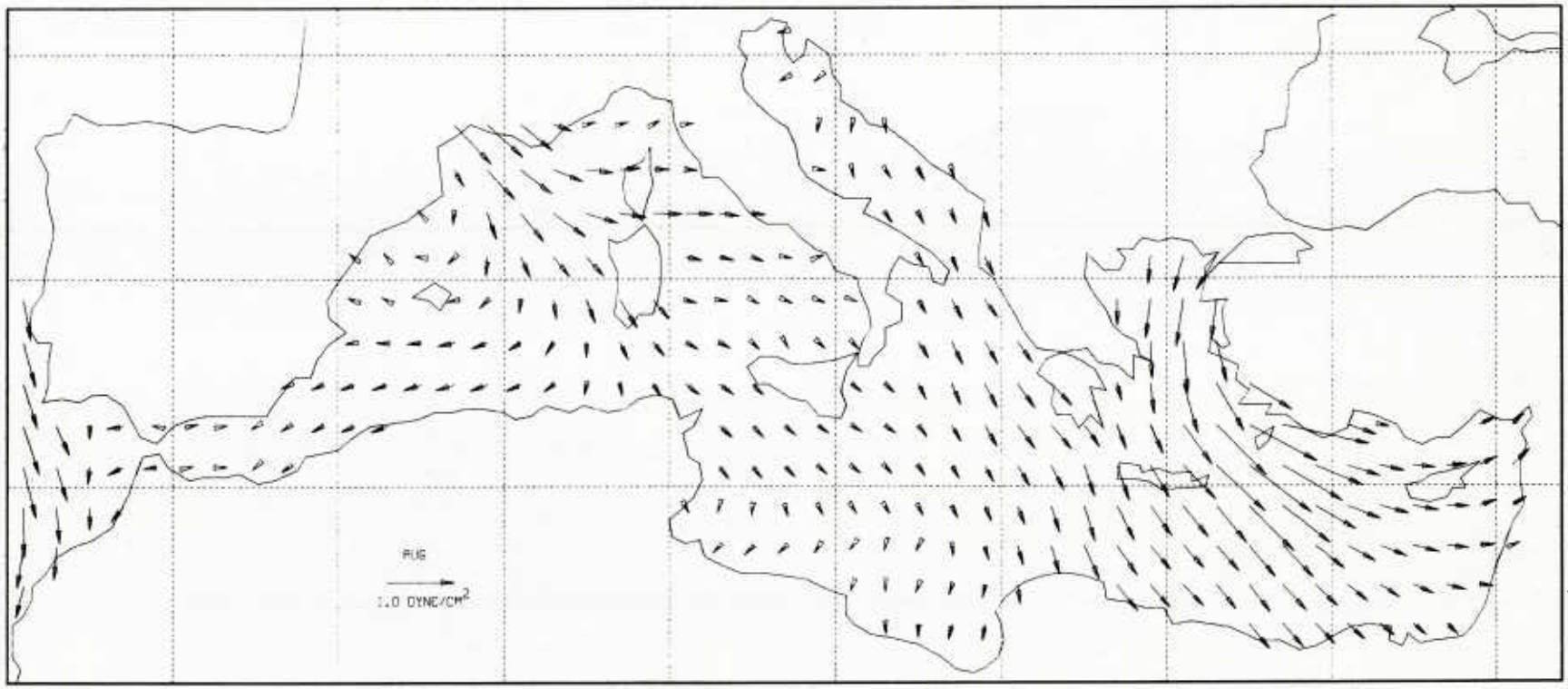

Figure A8. August wind stress (filtered)

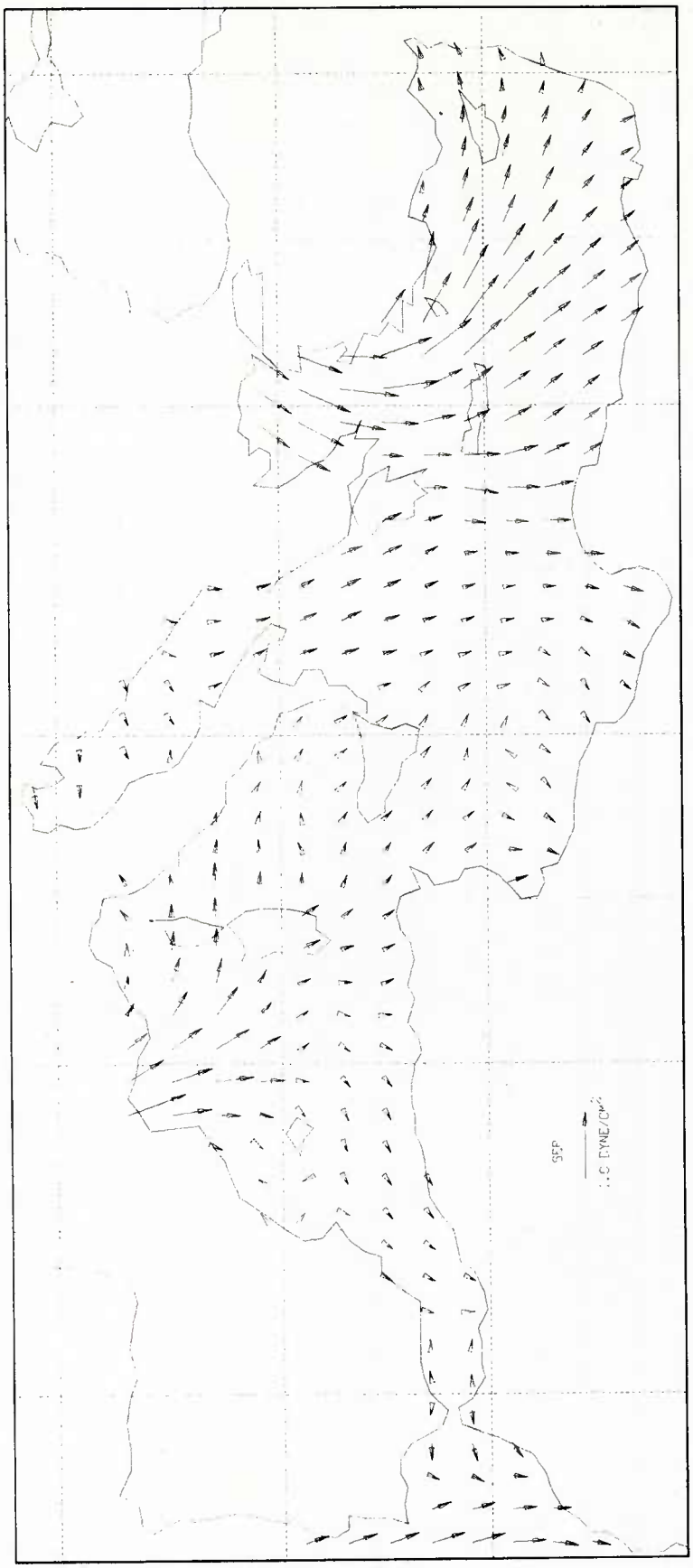

Figure A9. September wind stress (filtered)

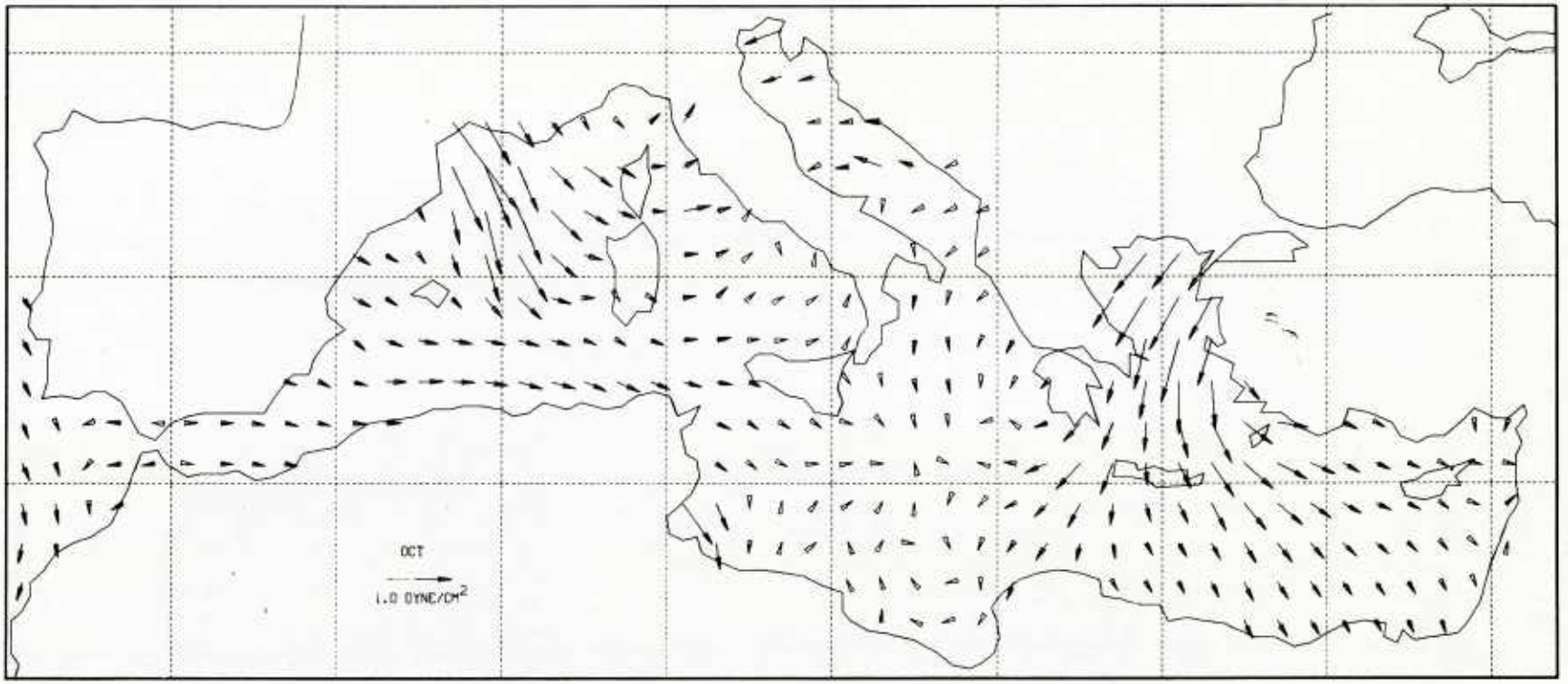

Figure A10. October wind stress (filtered)

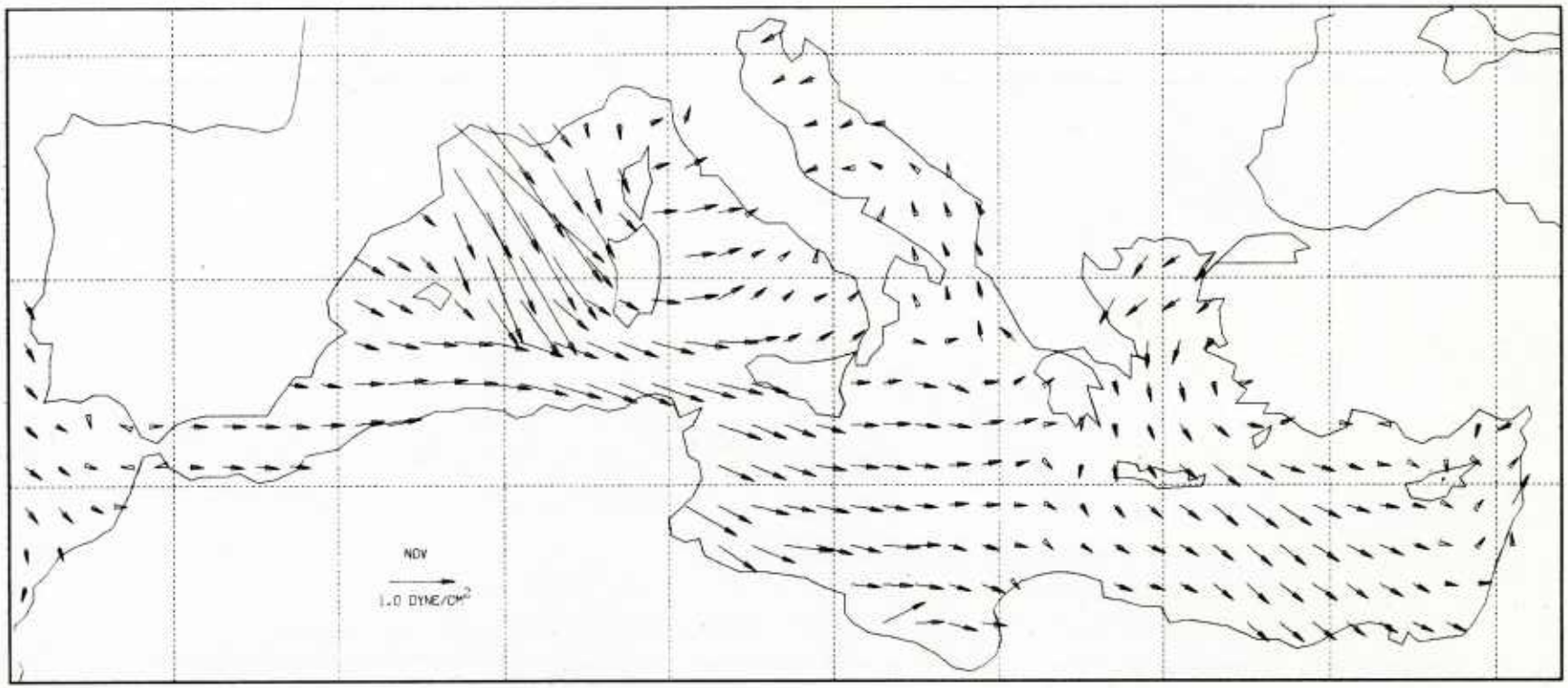

Figure A11. November wind stress (filtered)

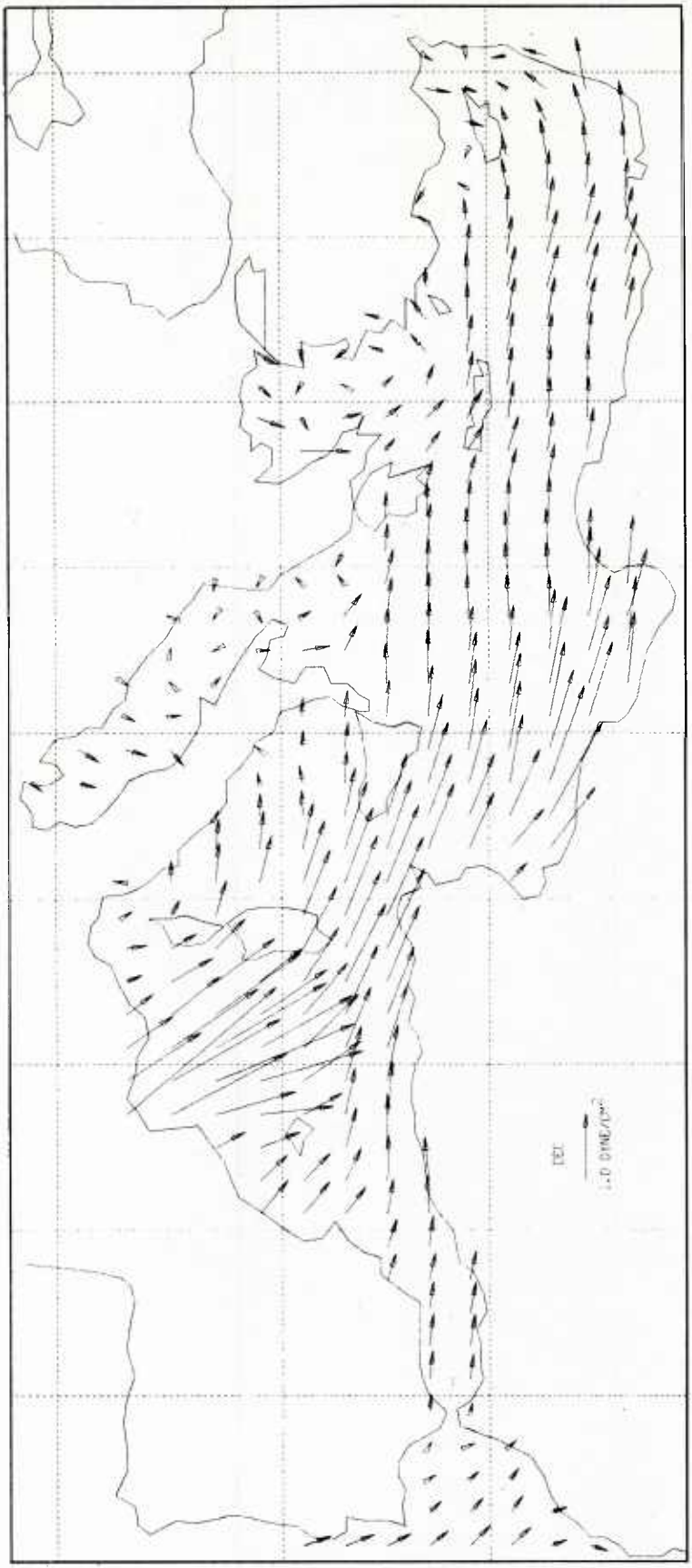

Figure A12. December wind stress (filtered)

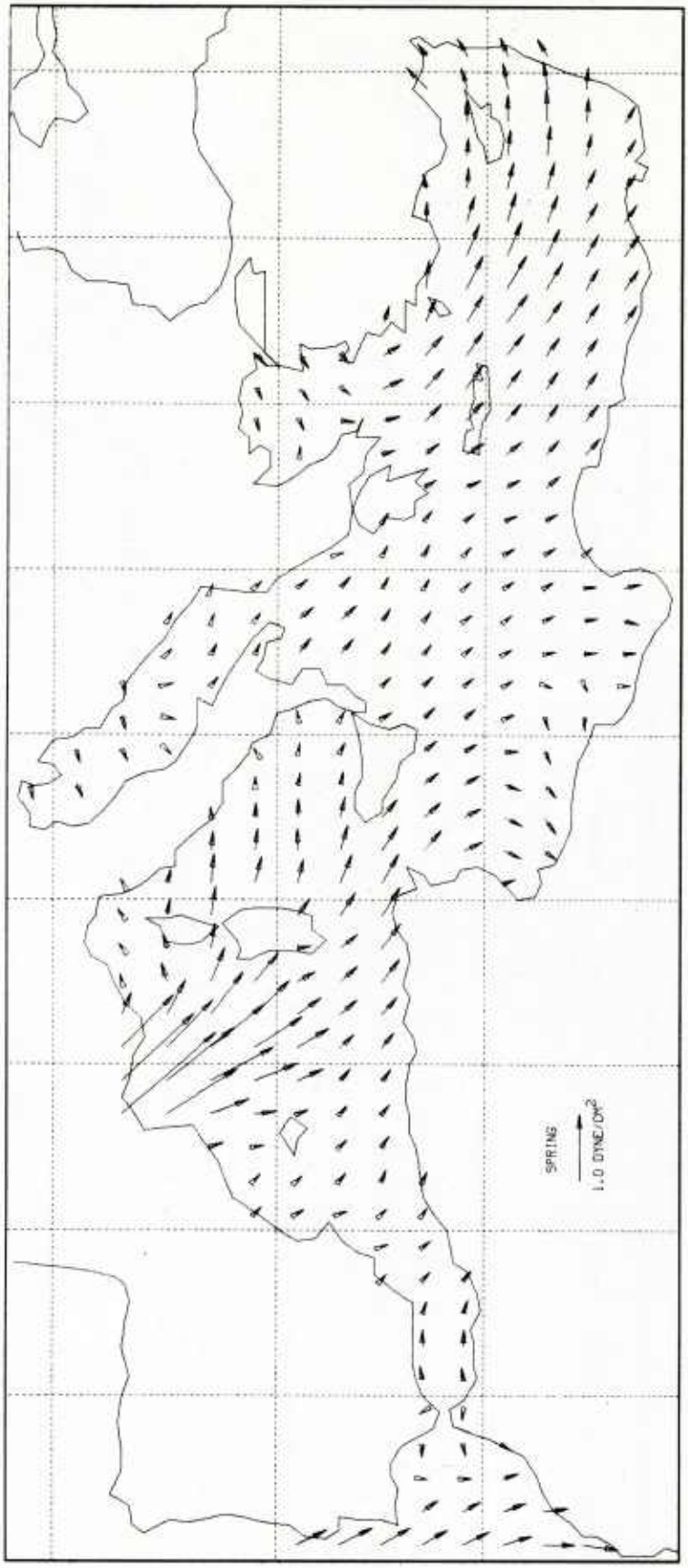

Figure A13. Spring wind stress (filtered)

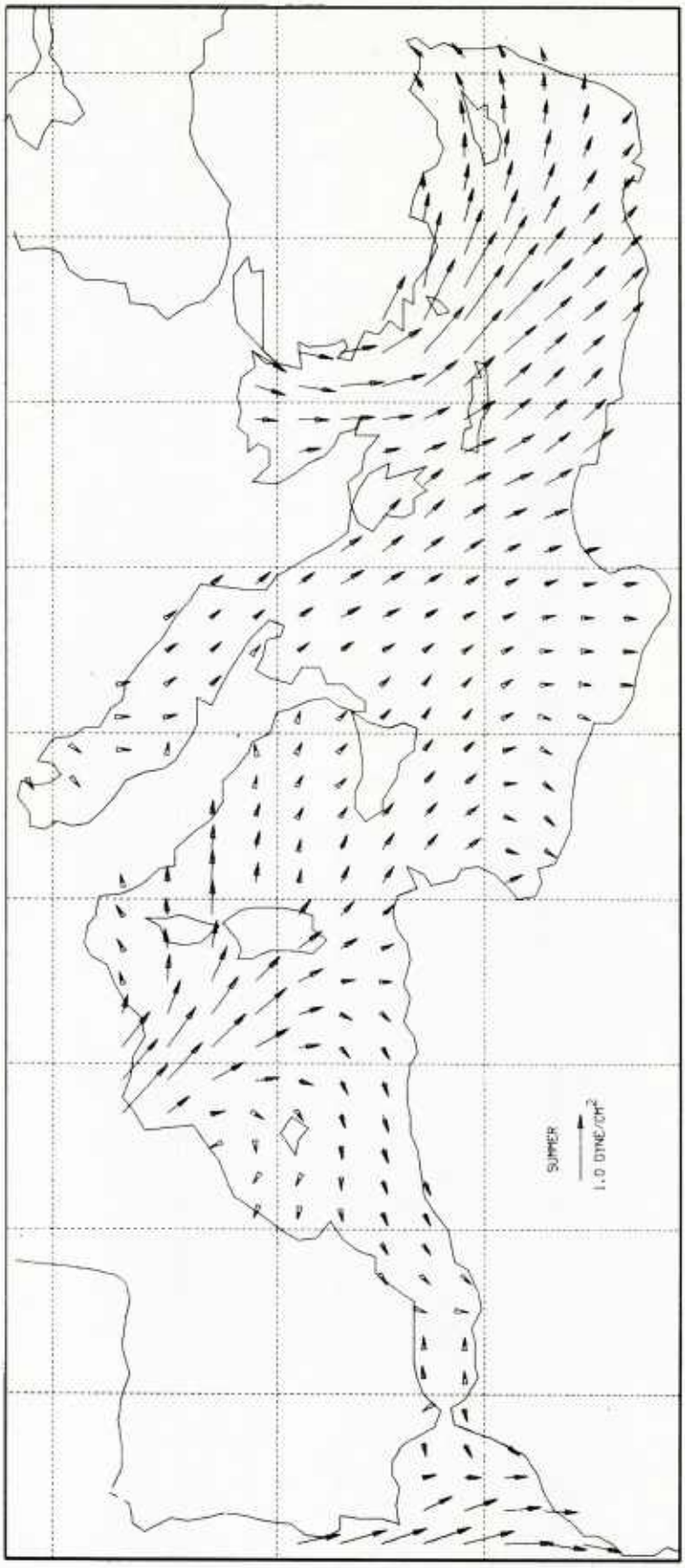

Figure A14. Summer wind stress (filtered)

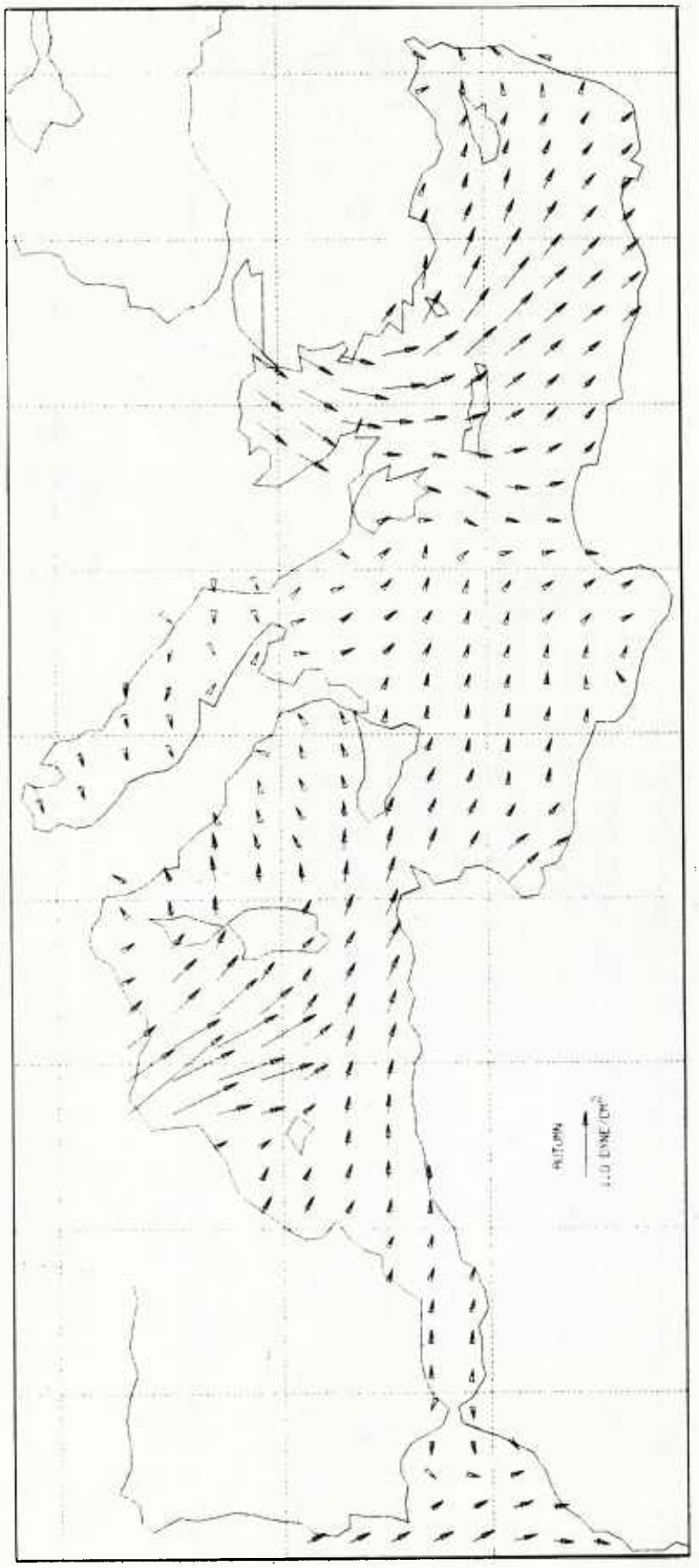

Figure A15. Autumn wind stress (filtered)

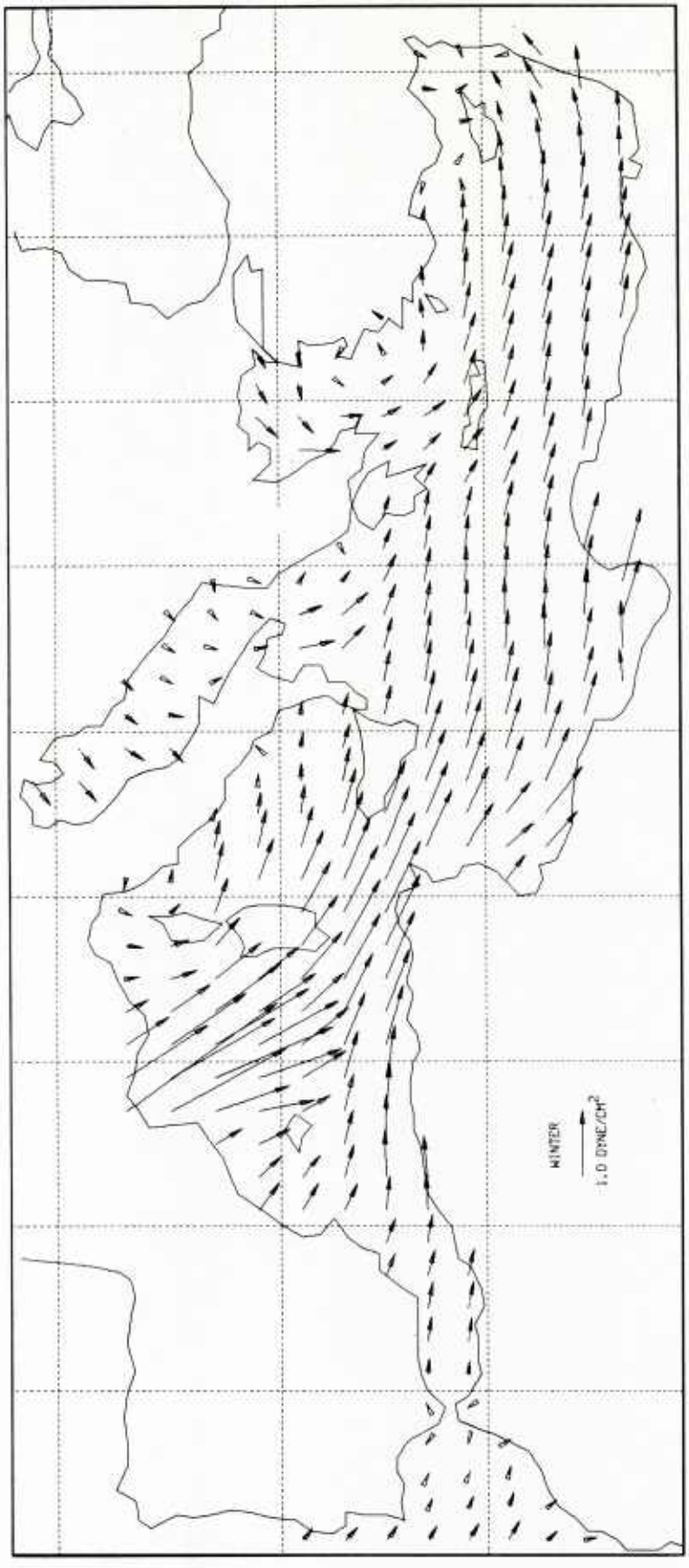

Figure A16. Winter wind stress (filtered)

DISTRIBUTION LIST (U)

Department of the Navy
Asst Secretary of the Navy
(Research Engineering & System)
Washington DC 20350

Project Manager
ASW Systems Project (PM-4)
Department of the Navy
Washington DC 20360

Department of the Navy
Chief of Naval Material
Washington DC 20360

Department of the Navy
Chief of Naval Operations
ATTN: OP 951
Washington DC 20350

Department of the Navy
Chief of Naval Operations
ATTN: OP 952
Washington DC 20350

Department of the Navy
Chief of Naval Operations
ATTN: OP 980
Washington DC 20350

Director
Defense Technology Info Cen
Cameron Station
Alexandria, VA 22314

Department of the Navy
Director of Navy Laboratories
Rm 1062 Crystal Plaza Bldg 5
Washington DC 20360

Commander
DWTaylor Naval Ship R&D Cen
Bethesda MD 20084

Commanding Officer
Fleet Numerical Ocean Cen
Monterey CA 93940

Commander
Naval Air Development Center
Warminster PA 18974

Commander
Naval Air Systems Command
Headquarters
Washington DC 20361

Commanding Officer
Naval Coastal Systems Center
Panama City FL 32407

Commander
Naval Electronic Sys Com
Headquarters
Washington DC 20360

Commanding Officer
Naval Environmental Prediction
Research Facility
Monterey CA 93940

Commander
Naval Facilities Eng Command
Headquarters
200 Stovall St.
Alexandria VA 22332

Commanding Officer
Naval Oceanographic Office
NSTL Station
Bay St. Louis, MS 39522

Commander
Naval Oceanography Command
NSTL Station
Bay St. Louis, MS 39522

Director, Liaison Office
Naval Ocean R&D Activity
800 N. Quincy Street
502 Ballston Tower #1
Arlington VA 22217

Commanding Officer
Naval Ocean R & D Activity
ATTN: Codes 110/111
NSTL Station MS 39529

Commanding Officer
Naval Ocean R & D Activity
ATTN: Code 125L
NSTL Station MS 39529

Commanding Officer
Naval Ocean R & D Activity
ATTN: Code 300
NSTL Station MS 39529

Commanding Officer
Naval Ocean R & D Activity
ATTN: Code 115
NSTL Station MS 39529

Commanding Officer
Naval Ocean R & D Activity
ATTN: Code 500
NSTL Station MS 39529

Commander
Naval Ocean Systems Center
San Diego CA 92152

Superintendent
Naval Postgraduate School
Monterey CA 93940

Commanding Officer
Naval Research Laboratory
Washington DC 20375

Commander
Naval Sea System Command
Headquarters
Washington DC 20362

Commander
Naval Surface Weapons Center
Dahlgren VA 22448

Commanding Officer
Naval Underwater Systems Center
ATTN: New London Lab
Newport RI 02840

Department of the Navy
Office of Naval Research
ATTN: Code 102
800 N. Quincy St.
Arlington VA 22217

Officer in Charge
Office of Naval Research
Detachment, Boston
Barnes Building
495 Summer St.
Boston, MA 02210

Commanding Officer
ONR Branch Office LONDON
Box 39
FPO New York 09510

Commanding Officer
ONR Western Regional Ofs
1030 E. Green Street
Pasadena CA 91106

Director
Scripps Inst of Oceanography
Univ of Southern California
La Jolla CA 92093

Working Collection
Texas A & M University
Department of Oceanography
College Station, TX 77843

President
Woods Hole Oceanographic Inst
Woods Hole, MA 20543